



Investigating Mechanical Properties of Metakaolin-Based Geopolymer Concrete Optimized with Wastepaper Ash and Plastic Granules

Midhin A. Khaleel Midhin^{1, 2*}, Leong Sing Wong^{1, 2}

¹Department of Civil Engineering, College of Engineering, Universiti Tenaga Nasional, Jalan IKRAM-UNITEN, 43000 Kajang, Selangor, Malaysia.

²Institute of Energy Infrastructure, Universiti Tenaga Nasional, Jalan IKRAM-UNITEN, 43000 Kajang, Selangor, Malaysia.

Received 25 August 2024; Revised 12 November 2024; Accepted 03 December 2024; Published 16 December 2024

Abstract

This study develops an environmentally friendly geopolymer concrete (GPC) using wastepaper ash (WPA) and high-density polyethylene (HDPE) granules, addressing environmental challenges such as wastepaper and HDPE disposal and CO₂ emissions from cement production. WPA was produced by incinerating wastepaper at 550 °C for one hour and used as a partial replacement for MK in ratios of 10%, 20%, 30%, 40%, 50%, and 100%, while HDPE granules replaced river sand in ratios from 1% to 5%. The results showed that the use of 30% WPA resulted in a compressive strength (CS) of 35.38 MPa, which was significantly higher than the control sample's CS of 31.62 MPa. The use of 30% WPA increased slump due to lower water demand. The combination of 3% HDPE and 30% WPA further enhanced the mechanical properties, resulting in a CS of 36.54 MPa, representing a 15.5% increase over the control. However, the addition of 3% HDPE and 30% WPA reduced the slump, attributed to the increased friction from the HDPE granules. Advanced analyses, including SEM, EDX, and XRD, confirmed a refined pore structure and increased geopolymerization in the treated GPC. It is novel to optimize WPA and HDPE as waste products in the production of MK-based GPC.

Keywords: Geopolymer Concrete; Wastepaper Ash; HDPE; Energy Saving; Waste Materials; Mechanical and Chemical Properties.

1. Introduction

The rapid expansion of the global population and the rising demand for advanced construction have heightened the dependence on PC, the most common construction material globally. The manufacturing of ordinary PC accounts for around 5% of total global greenhouse gas emissions and contributes about 30% of worldwide CO₂ emissions. Producing one ton of ordinary PC emits approximately 0.53 tons of CO₂ into the environment [1–3]. The substantial environmental impact has prompted urgent demands for the creation of sustainable alternatives with lower carbon footprints [4]. Geopolymer cement has evolved as an appropriate substitute to conventional PC, employing natural ingredients or industrial wastes and curing at ambient temperatures [5]. The chemical reaction of aluminosilicate-rich substances, such as MK, fly ash (FA), and GGBS, with an alkaline activator solution produces geopolymer cement. This method creates several solid phases, such as C-A-S-H, which makes the material better in terms of its microstructure, durability, and mechanical properties [6–8].

Wastepaper constitutes a substantial portion of worldwide solid waste, produced at a yearly rate of around 400 million tons from diverse sources, including newspapers and office documents [9–12]. Traditional disposal options, including incineration and landfilling, provide significant environmental issues, such as soil and water contamination and the

* Corresponding author: pe21231@student.uniten.edu.my

<http://dx.doi.org/10.28991/CEJ-SP2024-010-011>



© 2024 by the authors. Licensee C.E.J, Tehran, Iran. This article is an open access article distributed under the terms and conditions of the Creative Commons Attribution (CC-BY) license (<http://creativecommons.org/licenses/by/4.0/>).

exhaustion of land resources [13–15]. In considering these problems, researchers are progressively investigating efficient techniques for recycling waste materials, especially wastepaper [16, 17]. While cellulose in paper is non-toxic, the inks used may include hazardous compounds that pose environmental dangers [18]. The necessity of recycling highlights the possible economic and environmental advantages. Conventional recycling techniques have caused environmental harm, prompting the exploration of more sustainable alternatives [19, 20]. A viable strategy involves integrating waste byproducts, such as WPA, into construction materials [21]. Prior research suggests that the incorporation of paper sludge ash into geopolymer mortars can improve their mechanical properties [22–26]. Most studies have not explored the potential of WPA in geopolymer binders, particularly in relation to its impact on the characteristics of GPC. Although prior studies have examined the use of discarded paper in alternative concrete materials, such as papercrete and fibrous cement [27, 28]. Sadique et al. [27] investigated the production of papercrete using discarded office paper, highlighting its limitations, such as elevated water absorption and lower CS. Additionally, Solahuddin & Yahaya [16] investigated the incorporation of wastepaper fibers in fibrous cement. The absence of evaluation of WPA's potential in geopolymer binders in previous studies highlights the gap in the literature about the mechanical performance of GPC incorporated with WPA.

Recent studies have concentrated on the synergistic effects of employing various precursors in GPC, specifically emphasizing the combination of MK, GGBS, FA, and dolomite to improve mechanical quality and sustainability. Luo et al. [29] investigated the incorporation of 70% GGBS and 30% MK in self-compacting GPC, demonstrating significant enhancements in compressive and tensile strengths attributed to increased C-S-H production, resulting in a more compact microstructure. Gopalakrishna & Pasla [30] reported on ambient-cured geopolymer mortar consisting of 50% fly ash, 30% GGBS, and 20% MK, highlighting the ideal composition that enhanced pozzolanic reactions and mechanical properties. Thakur & Bawa [31] examined a composition consisting of 60% fly ash, 30% GGBS, and 10% dolomite in their GPC, revealing that this distinctive combination significantly improves strength and durability, particularly in terms of resistance to environmental challenges. The summarized results from these studies highlight the potential of customized precursor combinations to yield high-performance GPC, presenting a viable alternative to traditional cementitious materials while also minimizing environmental issues related to conventional concrete production.

Moreover, the building sector is a major source of emissions of greenhouse gases, representing approximately 36% of worldwide energy consumption and associated CO₂ emissions [32]. Cement and other construction materials constitute more than 90% of emissions associated with building activities [33, 34]. This problem intensifies due to the growing production of plastic waste, as only 9% of the estimated 100 million tons produced annually undergo recycling [34–39]. To mitigate climate change, the building industry must implement sustainable technologies and materials, including the recycling of waste resources [40]. Geopolymers, which are made up of materials that are high in aluminosilicates and are activated by alkaline solutions, could be used instead of regular cement [41]. HDPE is a promising reinforcing material owing to its chemical stability and resistance [42]. Research indicates that the integration of recycled HDPE into concrete can improve CS and diminish greenhouse gas emissions associated with plastic waste [43]. However, the impact of HDPE on GPC remains predominantly unexamined, as most studies concentrate on traditional concrete. Recent studies have highlighted the potential of using HDPE in GPC to improve mechanical qualities and promote sustainability. Atienza et al. [44] examined the integration of HDPE into foam fly ash geopolymers, concentrating on CS, density, and thermal conductivities. They emphasized that the incorporation of this material could enhance the mechanical properties of the geopolymer matrix, suggesting a necessity for additional investigation into HDPE's function in GPC. In a supplementary investigation, Tamil Selvi et al. [45] used HDPE as a partial replacement for coarse aggregate in traditional concrete at varying ratios of 1%, 2%, 3%, 4%, and 5%. Their findings indicated that substituting 3% of coarse aggregate with HDPE led to a substantial enhancement in CS, STS, and FS. This illustrates that even small amounts of HDPE can significantly enhance the mechanical qualities of GPC, in accordance with sustainability goals, by employing waste resources. These findings indicate that the inclusion of HDPE can improve the performance of GPC and promote ecologically sustainable construction methods.

The alkaline activator solution plays a vital role in geopolymerization by facilitating the formation of crystal structures, particularly those composed of silicon (Si) and aluminum (Al). Commonly, this solution consists of sodium hydroxide (NaOH) or potassium hydroxide (KOH), along with either sodium silicate (Na₂SiO₃) or potassium silicate (K₂O₃Si). Numerous researchers recognize that the alkaline activator solution is essential for beginning the polymerization reaction and that the incorporation of a silicate solution into NaOH and/or KOH facilitates the polymerization process. Zhang et al. [46] supported the theory by showing that solutions of NaOH and Na₂SiO₃ had higher CS than solutions of KOH and K₂SiO₃. Material safety categorizes alkaline compounds as either corrosive (harmful) or irritating (less harmful). Corrosive substances like NaOH and KOH necessitate careful handling with adequate protection, including gloves, safety glasses, and masks, especially in extensive applications [5]. Hydrated lime products, including calcium hydroxide (Ca(OH)₂), categorized as irritants, necessitate few protective measures and can be used in substantial quantities without excessive caution. These reagents classify in this category as "friendly" [5]. Yang et al. [47] evaluated GPC's mechanical properties with GGBS utilizing (Ca(OH)₂) as the principal activator at a concentration of 7.5% of the total binder. This was supplemented with Na₂ SiO₃ and sodium carbonate Na₂ CO₃ at concentrations of 1% and 2%, respectively. The results indicated that raising the water-to-binder (W/B) ratio adversely affected the CS of the GPC. The CS of mixtures including Ca(OH)₂ and Na₂ SiO₃ was higher than that of mixes

containing Na_2CO_3 . This study emphasizes the essential role of activator selection and curing techniques in improving the efficacy of GGBS-based GPC formulations.

The integration of WPA and HDPE in GPC significantly diminishes the environmental effect relative to conventional concrete during its lifecycle, primarily due to reduced CO_2 emissions during production, increased durability, and superior end-of-life recycling alternatives. In contrast to Portland cement, which is responsible for roughly 8% of global CO_2 emissions [48], the use of industrial by-products in GPC, such as wastepaper ash, thereby diminishes dependence on virgin raw materials and redirects waste from landfills [49]. The use of HDPE, especially recovered plastic, enhances sustainability by reducing plastic waste and encouraging a circular economy [50]. Furthermore, GPC demonstrates superior resistance to chemical degradation and enhanced durability, potentially reducing maintenance requirements [51], while its unique chemical composition allows for easier recycling than conventional concrete [52].

Based on these previous literature studies, there is a literature gap between the relevant application of WPA and HDPE and the enhancement in mechanical properties of MK-based GPC. This research targets the advancement of the creation of environmentally sustainable construction materials through the exploration of creative combinations, thereby reducing the ecological footprint of the construction sector. The advancement of sustainable GPC has attracted considerable attention, especially in substituting traditional materials with environmentally beneficial options. The theoretical structure focuses on the geopolymerization process, in which aluminosilicate precursors such as MK interact with alkaline activators to create a robust and resilient matrix. MK, as a highly reactive aluminosilicate, plays a vital role in the development of the geopolymer gel by providing silica and alumina, essential for forming a dense network of cross-linked bonds. The incorporation of WPA, characterized by its high calcium content, promotes the synthesis of the C-A-S-H gel, which combines with the geopolymer gel to improve mechanical strength and durability. The study involves creating a mixture of $\text{Ca}(\text{OH})_2$ and Na_2SiO_3 , which is essential for optimizing reaction kinetics and microstructure. $\text{Ca}(\text{OH})_2$ promotes the release of supplementary calcium ions, contributing to the synthesis of C-A-S-H gel, while Na_2SiO_3 acts as a source of soluble silica, enhancing the production of the geopolymer gel. In combination, these activators improve the binding characteristics, yielding a denser and more resilient matrix.

2. Material and Methods

GPC is developed utilizing a variety of raw materials, including MK, gravel, river sand, HDPE, WPA, Na_2SiO_3 , $\text{Ca}(\text{OH})_2$, and superplasticizer (SP). Figure 1 depicts these materials, which were purchased from Malaysian building supply companies. Kaolin Malaysia Sdn. Bhd. provides powdered MK Figure 1-a, while Fizlestari Plastic Sdn. Bhd. supplies HDPE granules with sizes less than 2 mm in diameter Figure 1-d. Local wastepaper from offices and residences in Kajang, Selangor, Malaysia, is collected and incinerated at 550°C for one hour. This method intends to produce finely amorphous WPA Figure 1-b, which is necessary for the reactivity required for GPC. As reported by Cordeiro et al. [53], high-temperature incineration is effective for creating high-quality ash, serving as a predominantly amorphous pozzolan. Table 1 highlights the basic characteristics of the main raw ingredients used in the creation of the GPC. Bulk density measurements show that WPA, at 563 kg/m^3 , falls between MK and $\text{Ca}(\text{OH})_2$. Its bulk density is similar to fly ash from pulp and paper mills, according to Cherian and Siddiqua [54]. WPA has a specific gravity of 2.41, which is lower than MK but higher than $\text{Ca}(\text{OH})_2$. Blaine fineness testing reveals that WPA has a lower value than MK and $\text{Ca}(\text{OH})_2$. HDPE granules have a bulk density of 935 kg/m^3 , a specific gravity of 0.95, and a water absorption of 0.01%. Na_2SiO_3 standards play an important role in maintaining consistent outcomes regarding strength and durability in GPC Figure 1-e. The SiO_2 and Na_2O levels in the Na_2SiO_3 solution were 32.5% and 16.5%, respectively, to ensure appropriate chemical reactions throughout the mixing and curing process. A total water percentage of 51% in Na_2SiO_3 (as presented in Table 2) is necessary to achieve the desired bonding and strength in the geopolymer combination. Superplasticizer Master Glenium PCE 8522 was used in this study to allow for a reduction in water content, which is necessary for making high-strength GPC Figure 1-f. In this study, white $\text{Ca}(\text{OH})_2$ powder with a purity level of 96% and a molarity of 74.10 g/mol was used, highlighting its crucial function in the binder production process Figure 1-c.

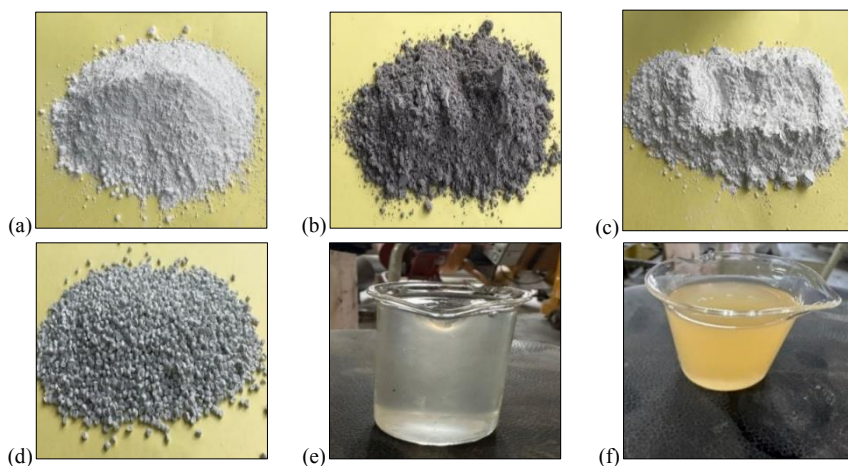


Figure 1. Images of the raw materials a) MK, b) WPA, c) $\text{Ca}(\text{OH})_2$ powder, d) HDPE granules, e) Na_2SiO_3 , f) superplasticizer

Table 1. Physical properties of the raw materials

Raw material	Basic properties			
	Bulk density (kg/m ³)	Specific gravity	Blaine fineness (cm ² /g)	Water absorption (%)
MK	1580	2.56	6631	-
WPA	563	2.41	2482	-
Calcium hydroxide	480	2.12	3189	-
HDPE	935	0.95	-	0.01
River sand	1337	2.55	-	1.27
Gravel	1588	2.49	-	0.83

Table 2. Chemical components of the raw materials

Chemical Composition	Percentage of weight (%)			
	MK	WPA	Sodium silicate	River sand
Aluminium oxide (Al ₂ O ₃)	40.8	20.200	-	1.470
Silicon dioxide (SiO ₂)	51.8	26.250	32.5	96.735
Phosphorus pentoxide (P ₂ O ₅)	1.67	0.565	-	-
Potassium oxide (K ₂ O)	0.228	0.542	-	0.295
Calcium oxide (CaO)	0.711	50.200	-	0.140
Titanium dioxide (TiO ₂)	3.13	0.285	-	0.015
Ferric oxide (Fe ₂ O ₃)	1.237	1.120	-	0.565
Zinc oxide (ZnO)	0.018	-	-	-
Gallium oxide (Ga ₂ O ₃)	0.03	-	-	-
Barium oxide (BaO)	-	0.028	-	-
ZrO ₂ (Zirconium (IV) oxide)	-	0.032	-	-
Strontium oxide (SrO)	0.089	-	-	-
Yttrium oxide (Y ₂ O ₃)	0.013	-	-	-
Zirconium dioxide (ZrO ₂)	0.263	0.038	-	-
Niobium (V) oxide (Nb ₂ O ₅)	0.011	-	-	-
Sodium oxide (Na ₂ O)	-	0.530	16.5	-
Vanadium(V) oxide (V ₂ O ₅)	-	0.01	-	-
Manganese (II) oxide (MnO)	-	0.038	-	-
Palladinite (PdO)	-	0.0524	-	-
Water (H ₂ O)	-	-	51	-
Loss on ignition	-	0.1096	-	0.78
Total weight (%)	100	100	100	100

2.1. Mix Design and Experimental Preparation

A comprehensive laboratory work plan was created to assess the properties of the GPC samples, as detailed in the flowchart presented in Figure 2. The control GPC mixture comprised 400 kg/m³ of MK, 240 kg/m³ of Na₂SiO₃, 160 kg/m³ of Ca(OH)₂, 732 kg/m³ of gravel, 366 kg/m³ of river sand, 8.4 kg/m³ of superplasticizer, and 420 kg/m³ of water, based on the published work by Midhin et al. [55] as specified in Table 3. The gravel exhibited a bulk density of 1588 kg/m³ and a specific gravity of 2.49, whereas the river sand had a specific gravity of 2.55 and a fineness modulus of 2.71, as seen in Table 1. The control GPC mixture had a water-to-solid binder ratio of 0.75, with a Na₂SiO₃ to Ca(OH)₂ ratio of 1.5. The dosage of superplasticizer was established at 1.5% of the total binder weight. The distribution of gravel particle sizes and river sand was assessed using the dry sieving method, while a particle size analysis was utilized to evaluate the size of MK and WPA particles. The sieve analysis results indicate that both sand and gravel conform to ASTM C33 [56] criteria, making them appropriate for construction use without modifications. The particle size analysis, depicted in Figure 3, demonstrated that MK exhibited smaller particles than WPA, hence enhancing their reactivity

during geopolymerization through improved contact with the alkaline activator, aggregates, and water in GPC. The specimen preparation conformed to standards, with designated methods of testing implemented for each mechanical property. The CS tests followed the standards of BS EN 12390-3:2019 [57], while the STS tests conformed to BS EN 12390-6:2009 [58]. FS tests were performed in accordance with ASTM C293M-16 (2016) [59], whereas UPV testing followed ASTM C597-16 [60] standards. Furthermore, ASTM C642-21 [61] was employed for water absorption testing, ensuring a precise assessment of the characteristics of the GPC samples. For the evaluations, we created cubes measuring 100×100×100 mm, and cylinders measuring 150×300 mm for CS testing, cylinders measuring 100×200 mm for STS testing, and prisms measuring 500×100×100 mm for FS testing. Non-destructive UPV testing was performed to evaluate the speed and duration of pulse transmission through the material, facilitating strength prediction, while water absorption tests measured the material's resistance to moisture penetration. The preparation and testing procedures were established to provide a comprehensive evaluation of the GPC's mechanical properties.

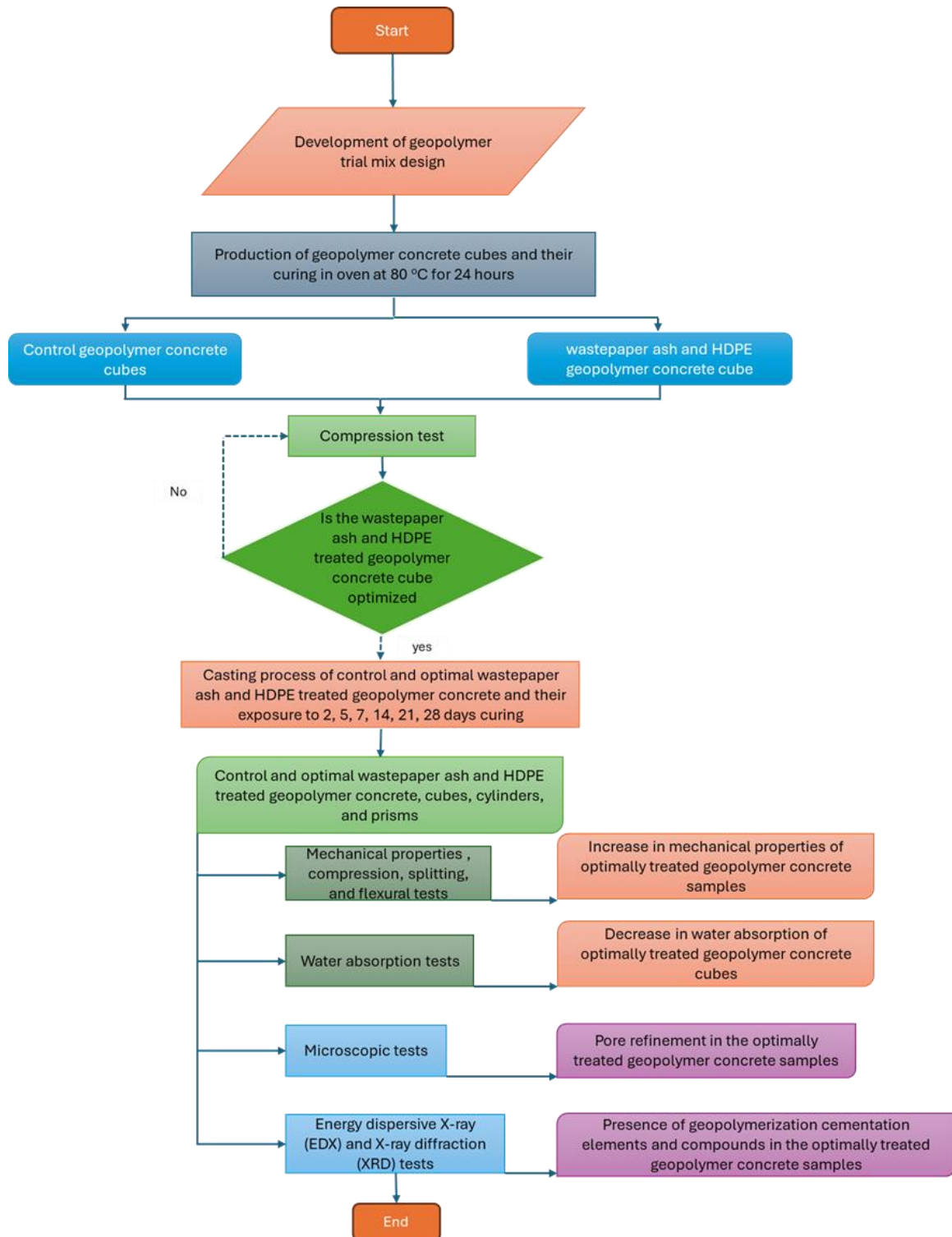


Figure 2. The flow chart of the experimental work

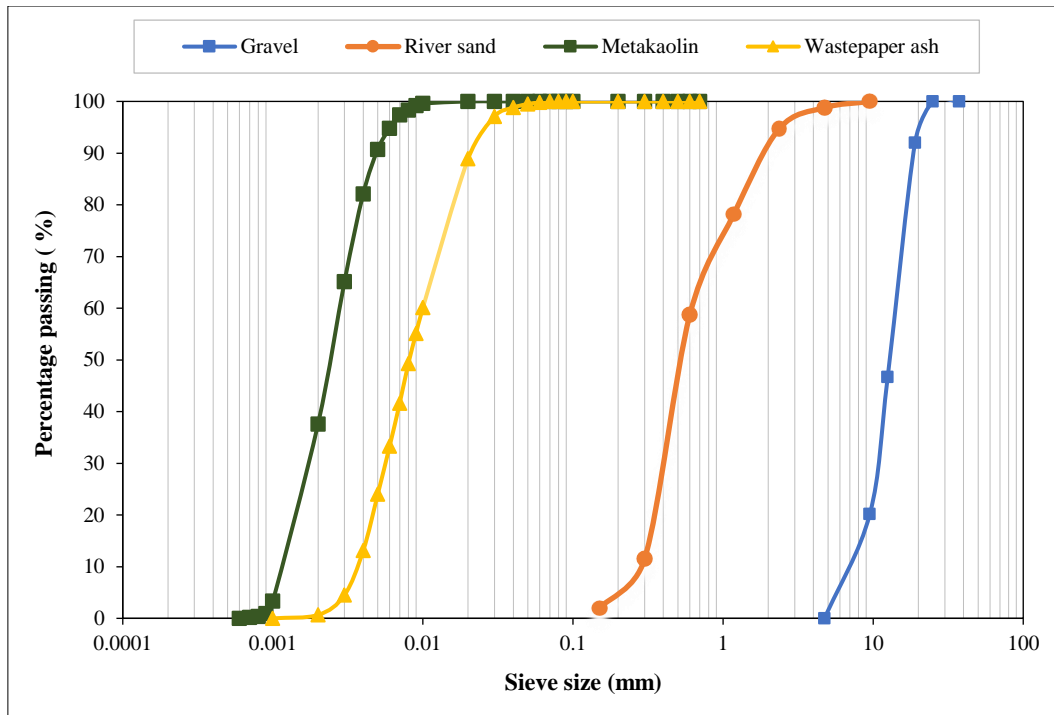


Figure 3. Particle size distribution curves of the raw materials

In the treated GPC, WPA was utilized to substitute MK at replacement rates of 10%, 20%, 30%, 40%, 50%, and 100%. Kumar et al. [62] found that the incorporation of GGBS in GPC permits a partial replacement of MK by up to 80%. Table 3 presents the proportions of raw materials used for the WPA GPC mixtures. GPC samples were made according to these mix designs (Figure 4-a) and were promptly covered with plastic film post-casting to avoid moisture. Following a 24-hour period, the samples were removed from their moulds, wrapped in aluminum foil, and then cured in a heated environment at 80°C for a further 24 hours (Figure 4-b). After heat treatment, the samples were removed from the oven (Figure 4-c), re-wrapped in plastic film, and preserved under ambient conditions until testing. The CS values were derived by averaging the findings from three samples for each mixture. Both the control and treated GPC samples were evaluated for CS using a universal testing machine, as illustrated in Figure 4-d. The composition with the highest 28-day average CS among the treated samples was identified as optimal. Thereafter, both the treated samples and the control samples were cast and cured for varying periods (2, 5, 7, 14, 21, and 28 days) post-heat treatment to observe CS development affected by the pozzolanic activity of WPA. After determining the optimal WPA content, substituted varying proportions of high-HDPE granules (1%, 2%, 3%, 4%, and 5%) for portions of river sand in the treated GPC. Table 4 highlights the mix designs with 30% WPA and differing HDPE percentages. The HDPE-modified mixture with the highest 28-day average CS was determined to be the most effective. Control and HDPE-treated GPC samples were subsequently cast and cured for 2, 5, 7, 14, 21, and 28 days following heat curing and evaluated for CS, STS, FS, and UPV. The treated GPC samples were analysed for water absorption in comparison to the control samples to measure water resistance. SEM analysis was conducted on both control and optimally treated samples to examine the pozzolanic effects garnered by the WPA. Furthermore, EDX and XRD investigations were performed to identify the elemental composition and mineral phases in the GPC samples.

Table 3. The trial mix proportion of the raw materials for designs of the WPA GPC in kg/m³

Sample name	MK	WPA	Na ₂ SiO ₃	Ca (OH) ₂	Gravel	Sand	Water	(SP)
WPA0 (Control) [55]	400	0	240	160	732	366	420	8.4
WPA10	360	40	240	160	732	366	420	8.4
WPA20	320	80	240	160	732	366	420	8.4
WPA30	280	120	240	160	732	366	420	8.4
WPA40	240	160	240	160	732	366	420	8.4
WPA50	200	200	240	160	732	366	420	8.4
WPA100	0	400	240	160	732	366	420	8.4



Figure 4. (a) the samples during casting, (b) the samples during steam oven curing, (c) the samples after casting, and (d) the Universal Testing Machine

Table 4. The trial mix proportion of the raw materials for designs of the treated GPC in kg/m³

Sample name	MK	WPA	Na ₂ SiO ₃	Ca (OH) ₂	Gravel	Sand	HDPE	Water	(SP)
HDPE0	280	120	240	160	732	366	0	420	8.4
HDPE1	280	120	240	160	732	362.34	3.66	420	8.4
HDPE2	280	120	240	160	732	358.68	7.32	420	8.4
HDPE3	280	120	240	160	732	355.02	10.98	420	8.4
HDPE4	280	120	240	160	732	351.36	14.64	420	8.4
HDPE5	280	120	240	160	732	347.7	18.3	420	8.4

3. Results and Discussion

The study begins with a wavelength dispersive X-ray fluorescence (WDXRF) assessment to identify the raw materials' chemical structure. The influence of WPA and HDPE on the bonding processes in treated GPC was examined by analyzing the 28-day peak CS findings. This comparison involved analyzing the partial substitution of MK with WPA and replacing river sand with HDPE granules at a microscopic level. The influence of curing on peak mechanical properties including CS, STS, and FS as well as water absorption was assessed for both control and treated GPC samples, revealing an enhancement in peak strength and a decrease in water penetration. According to Vu et al. [63], these results help set the characteristic CS, which is an important factor in the design of the structure and quality control of GPC. Wong et al. [64] and Wang et al. [65] have conducted prior research that highlights the importance of CS in enhancing the proportions of the concrete mix. The internal structure and chemical properties of both control and treated GPC specimens were examined at the microstructural level, including an investigation of common failure modes in GPC cylinders and their relationship with compressive stress-strain behavior. The following sections delve deeper into the detailed properties of the GPC samples, covering both macro- and micro-level observations to provide a comprehensive understanding of the material's performance.

3.1. WDXRF Analysis on the Used Precursor Materials

The chemical analysis of the raw materials was conducted utilizing WDXRF tests, with the results presented in Table 2. WDXRF analysis was conducted using a Rigaku Supermini 200 Spectrometer, recognized for its high-power benchtop sequential WDXRF capabilities, making it suitable for quantifying oxide components necessary for GPC synthesis. Analysis of MK oxide compounds demonstrated a silica-to-alumina ($\text{SiO}_2/\text{Al}_2\text{O}_3$) molar ratio of 1.27, signifying an adequate quantity of silicate for the geopolymerization process. Fletcher et al. [66] investigated geopolymer systems based on MK with varying $\text{SiO}_2/\text{Al}_2\text{O}_3$ ratios, from 0.5 to 300, and determined that the optimal ratio for strong development is $\text{SiO}_2/\text{Al}_2\text{O}_3 = 2$. Moreover, geopolymer mixtures with elevated Si content necessitated supplementary water, leading to the formation of hydrated Al species exhibiting octahedral coordination. Autef et al. [67] discovered that amorphous silica is essential for the development of the geopolymer structure.

The CaO and SiO_2 weights of WPA were found to be 50.200% and 26.250%, respectively, indicating a CaO/ SiO_2 molar ratio of 1.912 and demonstrating its pozzolanic properties. Meko & Ighalo [68] discovered that WPA included 50.88% CaO and 29.20% SiO_2 , with a slightly lower CaO/ SiO_2 molar ratio of 1.742. Such a comparison implies that paper ash is pozzolanic in nature. The high calcium content (50.200%) of WPA results in the development of strong C-A-S-H gels. Adesanya et al. [23] reported additional evidence of the pozzolanic activity generated by paper sludge ash in geopolymer cement. This value is significant because it is comparable to the CaO concentrations typically found in GGBS, a widely utilized supplementary cementitious material in GPC production. Prior research has indicated that CaO contents in GGBS vary between 39.23% and 52.69% [69-72]. The comparable CaO content highlights the pozzolanic capability of WPA, indicating its effectiveness in facilitating the formation of robust (C-A-S-H) gels, essential for improving the mechanical properties of the resultant GPC. The presence of heavy metal compounds, including 0.01% V_2O_5 , 0.038% MnO, 0.285% TiO_2 , 0.028% BaO, 0.038% ZrO_2 , and 0.0524% PdO, illustrates the harmful effects of WPA. The major component of the river sand was quartz, demonstrated by its SiO_2 composition of 96.735% by weight.

3.2. Fresh Properties and Setting Time

This section summarizes the findings of slump tests conducted to assess the water content, consistency of GPC, and setting times. The experiment employed three different types of GPC: 100% MK, a mixture of 70% MK and 30% WPA, and a mixture of 70% MK, 30% WPA, and 3% HDPE. Workability assessments were conducted by mixing each batch with fresh GPC. The slump test is an essential method for assessing the fluidity and workability of GPC mixes. Figure 5 illustrates that the incorporation of 30% WPA and 3% HDPE influences the slump results of GPC. The slump increases by 8.86% when 30% WPA is incorporated, reaching 86 mm, compared to 79 mm with 100% MK [55]. The increase may be ascribed to the lower fineness modulus of WPA compared to MK, demanding less water and enhancing the workability of GPC. This result aligns with a recent work on slag/fly ash blends [73, 74], which indicated that the large surface area of slag necessitates much water, leading to reduced slump. The incorporation of 3% HDPE into a mixture containing 30% WPA led to a 4.65% decrease in slump, reducing it to 82 mm, in contrast to the mixture containing only 30% WPA. The roughness of HDPE particles and their large surface area, which facilitates significantly reduced workability, may be the cause of this reduction. Prior studies focusing on polyethylene terephthalate (PET) and recycled plastic in concrete [75, 76] confirm this. The results align with the studies by Jindal et al. [77] and Waqas et al. [78], which found that substituting fly ash with 30% GGBS yields a low slump value.

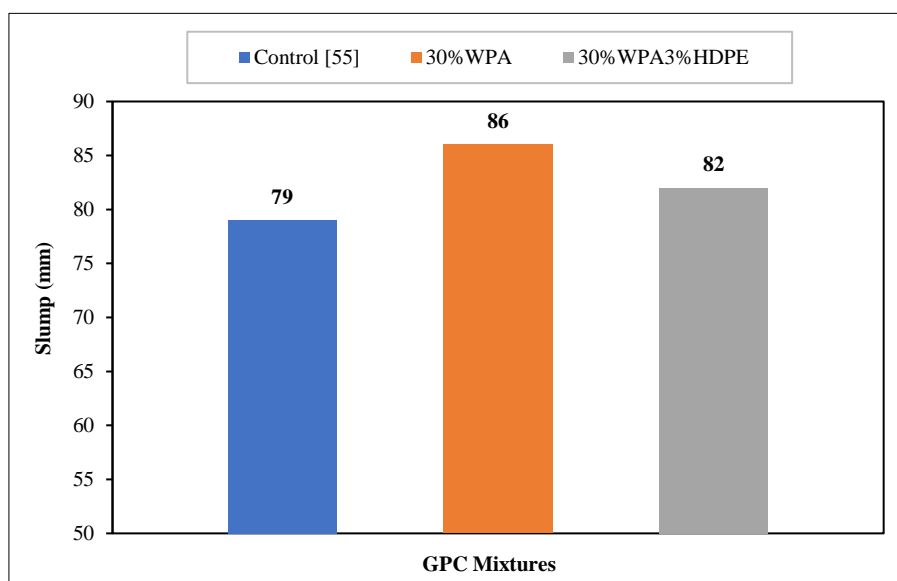


Figure 5. The slump test results of different geopolymer concrete mixtures

Figure 6 presents the results of the time-setting assessment for GPC paste, which used varying amounts of MK and 30% WPA. Incorporating 30% WPA into the geopolymer mixture significantly enhances setting times, yielding a 11 % reduction in the initial setting and a 28.5% reduction in the final setting. The MK geopolymer blend exhibits initial and final setting periods of 18 and 70 minutes [55], respectively; however, the incorporation of 30% WPA reduces the periods to 16 and 50 minutes, respectively. WPA in the GPC mixture induces rapid solidification, which significantly enhances performance. The elevated CaO concentration in WPA relative to MK is the primary reason for this enhancement. Research by Xie et al. [79] and Lee et al. [80] suggests that the presence of CaO serves as an effective heterogeneous nucleation site inside the paste, thereby expediting the setting process. The catalytic effect of CaO significantly reduces the setting time of GPC paste, emphasizing the enhanced performance characteristics obtained with the addition of WPA. The combination of MK and 30% WPA significantly changes the setting behavior of the geopolymer mixture, suggesting an effective approach to enhancing the time-setting properties of GPC formulations. The results underscore the essential role of WPA in facilitating rapid solidification; hence, accelerating the setting process and enhancing the overall effectiveness of GPC paste. Hadi et al. [81] observed that the inclusion of 40% GGBS with a high CaO content in GPC yielded initial and final setting times of 33 and 58 minutes, respectively. The results indicated that elevating the GGBFS content can significantly accelerate the setting of geopolymer pastes [82].

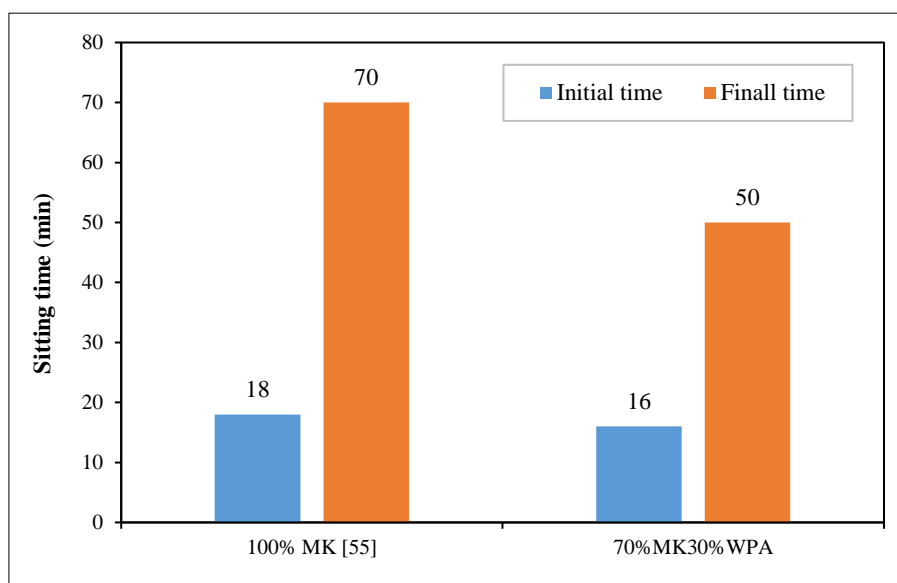


Figure 6. Initial and final setting time of different geopolymer concrete mixtures

3.3. Effect of Partial MK Replacement with WPA on the CS of the GPC

This section examines the impact of substituting MK with WPA on CS. The replacement of 10% WPA for MK in GPC was comprehensively assessed, with the findings illustrated in Figure 7. The figure demonstrates the effect of this substitution on the CS of GPC samples at various ages. The data clearly show that substituting MK with 10% WPA yields significantly higher CS compared to control samples [55]. The CSs at ages 2, 5, 7, 14, 21, and 28 days were 16.3 MPa, 20.22 MPa, 25.1 MPa, 26.73 MPa, 30.73 MPa, and 33.25 MPa, respectively. The CS of the 10% WPA samples exceeded that of the control samples by 10.5%, 7.5%, 7.3%, 7.7%, 9.3%, and 5% at the corresponding ages, respectively. Moreover, the findings indicate that the incorporation of 20% WPA yields superior CS compared to samples with 10% WPA. After two days, the CS of the GPC with 20% WPA was 16.62 MPa, indicating a 2% increase compared to the samples with 10% WPA. The trend continued throughout the curing period, yielding strengths of 21.13 MPa at 5 days, 25.44 MPa at 7 days, 27.65 MPa at 14 days, 31.47 MPa at 21 days, and 34.12 MPa at 28 days. These findings underscore the substantial impact of enhancing WPA substitution on CS of GPC. Moreover, the findings indicate that 30% WPA yields superior CS compared to 20% WPA. The GPC with 30% WPA had a CS of 17.2 MPa after two days, which is 3.48% higher than the samples with 20% WPA. The enhancement continued over time, achieving 21.78 MPa after 5 days, 25.88 MPa after 7 days, 29.3 MPa after 14 days, 33 MPa after 21 days, and 35.38 MPa after 28 days of curing. The 30% WPA samples had significantly elevated CS compared to the control samples, with increases of 16.7%, 15.8%, 10.7%, 18%, 17.4%, and 12% at the corresponding ages, respectively. The elevated concentration of calcium oxide in WPA is primarily responsible for the noted rise in CS.

Poloju & Srinivasu [83] reported that high levels of CaO make it easier for C-A-S-H gels to form quickly in GPC. Moreover, the combination of WPA and MK with $\text{Ca}(\text{OH})_2$ enhances the synthesis of calcium compounds, yielding a more compact geopolymer microstructure comprising C-A-S-H, C-S-H, and N-A-S-H gel. This leads to a significant rise in CS [74, 79, 80, 83]. The interaction of SiO_2 and Al_2O_3 in MK, along with SiO_2 , Al_2O_3 , and CaO in WPA and an alkali activator solution, facilitated the formation of N-A-S-H and C-A-S-H gels in GPC, as reported by Pawluczuk et

al. [84]. The formulation of these gels results in enhanced CS. The activation effect of Ca^{2+} enhanced the polymerization of GPC as the proportion of WPA binder increased, leading to elevated CS at an early age. Comparing the findings to earlier research, Shilar et al. [85] found that adding up to 30% GGBS, which is high in calcium oxide (CaO), to MK increased the CS of GPC. This was mostly due to the creation of a hybrid gel system with C-A-S-H and N-A-S-H. The C-A-S-H gel plays a crucial role in filling the gaps in the matrix, leading to a decrease in porosity and an increase in load-bearing capacity and thereby significantly enhancing the overall strength of the GPC. Elevated CaO levels accelerate the geopolymerization process, enhancing early-age strength development and making GGBS-enhanced GPC suitable for applications that demand rapid strength gain, like precast elements. Consequently, the use of CaO-rich GGBS enhances its mechanical properties while also improving the durability and service life of GPC.

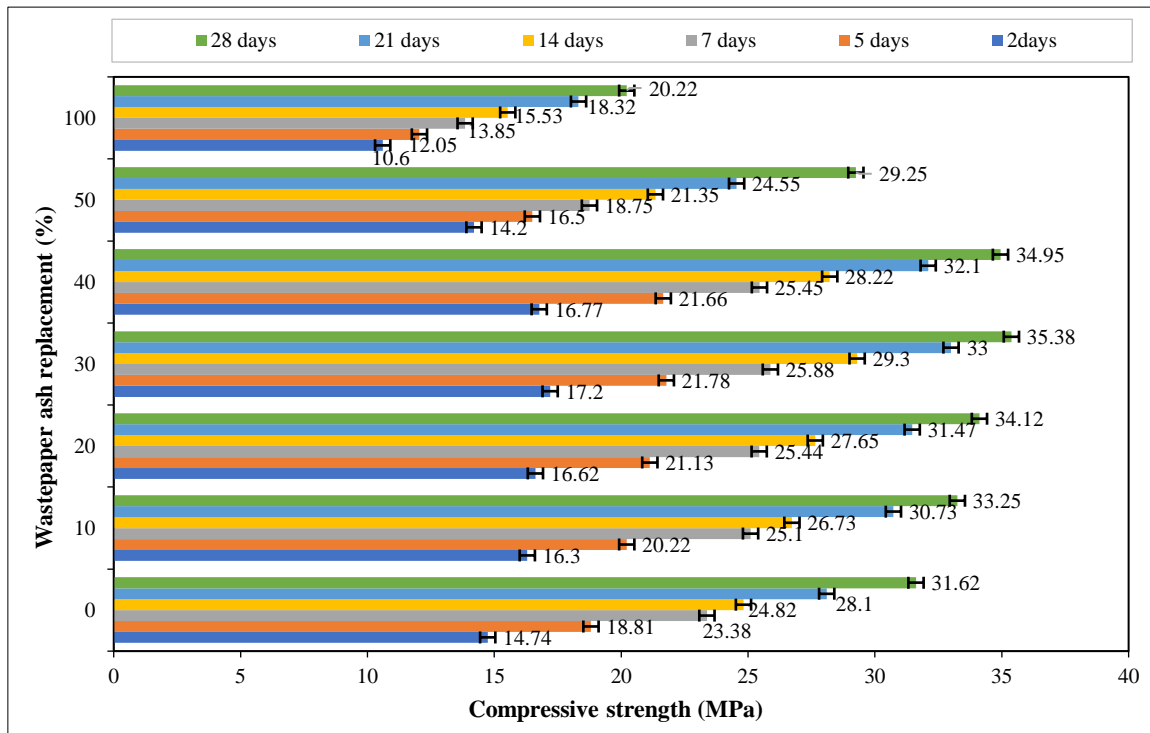


Figure 7. Effect of WPA as a replacement of MK on the CS of the GPC

The findings indicate that the incorporation of 40% WPA yielded CSs of 16.77 MPa, 21.66 MPa, 25.45 MPa, 28.22 MPa, 32.1 MPa, and 34.95 MPa after 2, 5, 7, 14, 21, and 28 days, respectively. Throughout these periods, the CS of the 40% WPA samples was slightly lower by 2.5%, 0.55%, 1.66%, 3.68%, 2.73%, and 1.21% compared to the 30% WPA samples. The 40% WPA samples demonstrated better CS values compared to the control samples and those with 10% and 20% WPA. The reduced CS observed with 40% WPA replacement, as compared to 30% WPA, can be attributed to an increased quantity of WPA in the geopolymer mixture, leading to a higher concentration of CaO. The elevated CaO concentration in the mixture may destabilize the $Na_2O-CaO-SiO_2-Al_2O_3-H_2O$ gel and hinder the production of C-A-S-H, leading to weaker bonds and a slight reduction in strength [86, 87]. Using 50% WPA yielded CSs of 14.2 MPa, 16.5 MPa, 18.75 MPa, 21.35 MPa, 24.55 MPa, and 29.25 MPa after 2, 5, 7, 14, 21, and 28 days, respectively. In contrast to the 30% WPA samples, the 50% WPA samples exhibited significant CS losses, varying from 17.3% to 27.55% over similar time periods. Additionally, the complete substitution of WPA resulted in a considerable reduction in CS, yielding values of 10.6 MPa, 12.05 MPa, 13.85 MPa, 15.53 MPa, 18.32 MPa, and 20.22 MPa at 2, 5, 7, 14, 21, and 28 days, respectively. The reductions were 28%, 35.94%, 40.76%, 37.43%, 34.80%, and 36%, respectively, in comparison to the control samples. The elevated concentration of WPA in the geopolymer mixture, which hinders the development of essential hydrates while introducing excess CaO, is responsible for the significant reduction in CS with 100% WPA substitution. The additional CaO accelerates the deterioration of the aluminosilicate structure, leading to a comprehensive decline in CS. The lower strength values seen in the test samples compared to the control show that the bond between the geopolymer combination's parts is getting weaker. The replacement of MK with 100% WPA may improve the generation of C-S-H gels in the geopolymer system due to the higher Ca^{2+} content, which has a lower strength than C, N-A-S-H gels, resulting in a decline in CS [88-90].

The results demonstrate that replacing MK with 30% activated WPA yields the maximum CS for GPC. This improvement is mainly due to the optimal balance of pozzolanic activity and binder properties that WPA provides at this specific ratio. At a 30% replacement level, significant chemical reactions occur, resulting in the synthesis of essential gel components, including C-A-S-H and N-A-S-H. These gels are crucial for enhancing the GPC's microstructure, resulting in increased density and reduced porosity, which are critical for strengthening the material's load-bearing capability.

3.4. Effect of Partial River Sand Replacement with HDPE Granules on the CS of the GPC

This section examines the impact of replacing river sand with HDPE granules on CS. The experimental findings for the CS data are presented in Figure 8. The study indicates that incorporating 1% HDPE into a mixture containing 30% WPA and 70% MK influences CS. Thus, substituting river sand with 1% HDPE results in a slight rise in CS. The CS values at 2, 5, 7, 14, 21, and 28 days were 17.6 MPa, 21.1 MPa, 26.25 MPa, 29.8 MPa, 33.4 MPa, and 35.63 MPa, respectively. The percentage improvements in CS for samples containing 1% HDPE were as follows: 2 days (2.3%), 5 days (1.5%), 7 days (1.4%), 14 days (1.7%), 21 days (1.2%), and 28 days (0.7%) compared to samples without HDPE. The results demonstrate that using 1% HDPE as a replacement for river sand enhances CS over time. Tamil Selvi et al. [45] discovered that substituting 1% HDPE for coarse aggregate in concrete enhanced the 28-day CS by 3.19%. Moreover, the incorporation of 2% HDPE yielded a 28-day CS of 36.12 MPa, indicating a 2.1% enhancement compared to samples without HDPE at the same age. This indicates that 2% HDPE yields a greater enhancement in CS compared to 1% HDPE. The CSs at 2, 5, 7, 14, 21, and 28 days were 18 MPa, 22.3 MPa, 26.25 MPa, 30.1 MPa, 33.8 MPa, and 36.12 MPa, respectively. Moreover, the findings indicate that 3% HDPE enhances CS more effectively than 1% and 2% HDPE. The CSs at 2, 5, 7, 14, 21, and 28 days were 18.2 MPa, 22.7 MPa, 26.8 MPa, 30.51 MPa, 34 MPa, and 36.54 MPa, respectively. The enhancement percentages for samples containing 3% HDPE compared to those without HDPE were: 2 days (5.8%), 5 days (4.22%), 7 days (3.55%), 14 days (4.1%), 21 days (3%), and 28 days (3.27%). The results agree with the studies conducted by Tamil Selvi et al. [45], indicating that a 3% substitution of HDPE enhances the CS of concrete. This agreement verifies that the inclusion of up to 3% HDPE enhances the CS of GPC.

The capacity to maintain load application, which promotes the transformation of shear stress into tensile stress, is responsible for this enhancement and the inclusion of plastic ultimately reinforces the concrete [75, 91]. The inclusion of 4% HDPE diminishes CS relative to 3% HDPE. At 2, 5, 7, 14, 21, and 28 days, the CS measured 17.65 MPa, 21.7 MPa, 26.1 MPa, 29.9 MPa, 33.5 MPa, and 35.75 MPa, respectively. Furthermore, the incorporation of 5% HDPE significantly reduced the CS compared to the addition of 3% HDPE. The CSs at various ages (2, 5, 7, 14, 21, and 28 days) were 16.75 MPa, 20.65 MPa, 25.3 MPa, 29.1 MPa, 32.15 MPa, and 34.92 MPa, respectively. A comparison of samples with 5% and 3% HDPE demonstrated CS losses of 7.96, 9, 3.73, 4.6, 5.44%, and 4.43% at 2, 5, 7, 14, 21, and 28 days, respectively. The reduction in CS with high HDPE substitution is attributable to the enhanced smoothness of the HDPE particles, which diminishes the adhesive strength between the geopolymer matrix and the HDPE particles. The findings of Dawood et al. [75] and Rahim et al. [91] confirm this result. Additionally, Shanmugapriya & Santhi [92] and Kangavar et al. [93] have demonstrated that adding more HDPE and PET to concrete lowers its unit weight, which in turn lowers its CS. A 3% HDPE replacement exhibits a notable improvement in CS. The elongation and stress conversion characteristics of HDPE significantly improve the strength of GPC, making it a suitable material for sustainable construction.

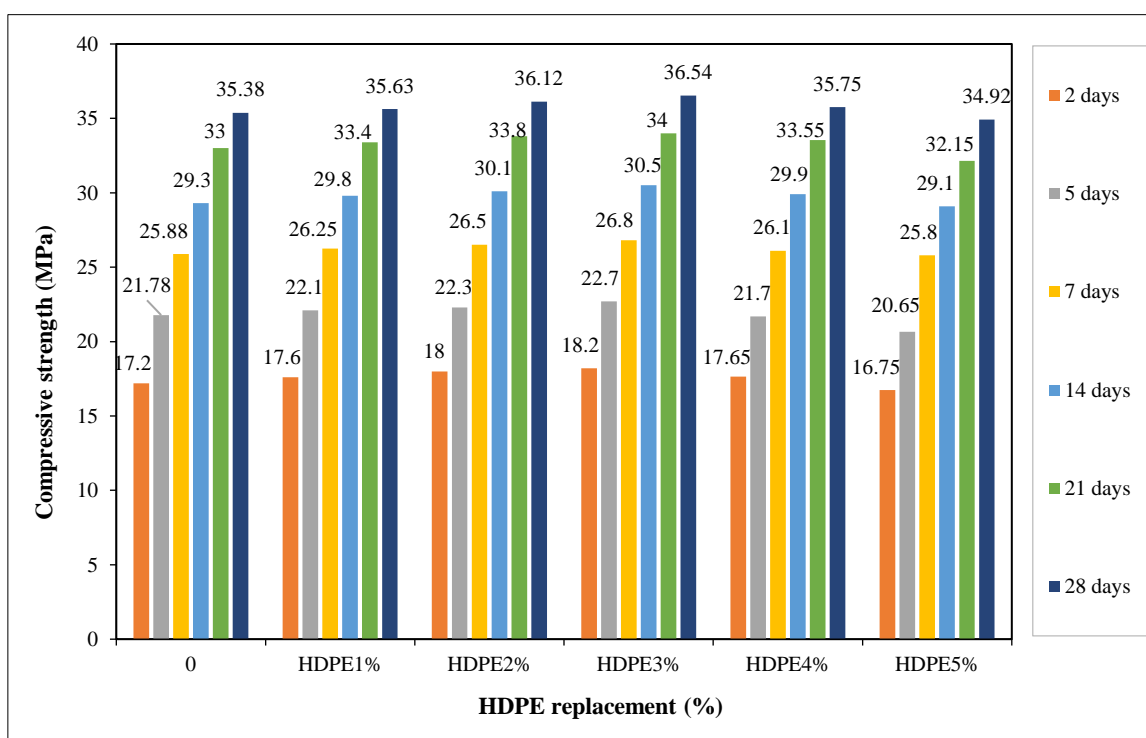


Figure 8. Effect of HDPE as a replacement of river sand on the CS of the GPC

The large-scale production and utilization of GPC includes WPA and HDPE for industrial and commercial purposes is feasible; however, several challenges must be overcome for successful commercialization. A primary obstacle is the absence of standardization and regulatory acceptance, as existing building codes mainly focus on conventional PC-based materials. To address this matter, it is essential that regulatory agencies, industry stakeholders, and researchers collaborate to develop standards specifically for geopolymer technology. Furthermore, the variability in raw material characteristics, especially WPA, highlights the need for consistent sourcing and processing methods to achieve reliable performance. Educational efforts and demonstration programs can significantly improve public perception as well as understanding of the environmental advantages of GPC. Although the initial costs of sourcing and processing WPA and HDPE might be higher, focusing on the long-term sustainability benefits and potential reductions in maintenance costs can help mitigate this concern. Addressing these challenges can significantly increase the commercial potential of GPC with WPA and HDPE across various applications.

3.5. STS of Control and Treated GPC

The study investigated the effect of treated GPC on STS. Figure 9 shows the STS results for both the control and treated samples. The findings indicate that combining 30% WPA and 3% HDPE has a similar effect on the CS and STS of GPC. The examination of treated GPC on STS indicates substantial improvements due to the synergistic integration of WPA and HDPE. The results show that the STS values for control samples were 2.52 MPa after 7 days and 3.35 MPa after 28 days. On the other hand, the STS values for treated samples were 2.85 MPa and 3.83 MPa, which are 13.1% and 14.32% higher, respectively. Both WPA and HDPE particles provide increased ductility, which primarily contributes to the significant improvement in STS. Adding WPA to the GPC matrix improves the pozzolanic reactions and creates a more refined microstructure with better bonding and fewer voids, which leads to better load distribution [91, 92]. Furthermore, the function of HDPE is crucial, as it mitigates slippage during loading conditions, effectively gathering fractures and enhancing energy absorption [75]. This dual-action process enhances the resilience of GPC structures, enabling them to withstand tensile pressures and consequently enhancing overall structural integrity. The enhancement of STS is essential for the performance and durability of GPC, particularly under bending and tensile stresses, as it improves the material's resilience to cracking and deformation [75, 92]. The relationship between STS and the material's stress resistance highlights the necessity of optimizing GPC formulations for advanced building applications. The synergistic effects of WPA and HDPE enhance STS and promote sustainable practices in polymer concrete manufacturing through the efficient use of waste materials.

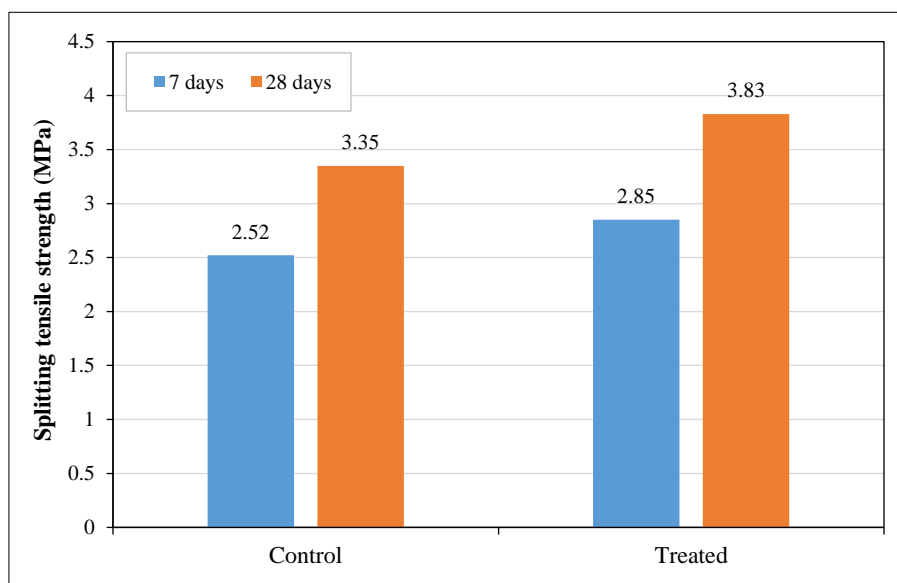


Figure 9. Effect of the treated GPC on the STS

3.6. FS of Control and Treated GPC

FS, a critical characteristic of GPC, evaluates its resistance to bending or tensile stresses. This is particularly crucial for building elements such as beams and slabs that are subject to bending pressures. Enhancing the FS of GPC significantly enhances its capacity for resisting cracking and deformation, hence improving its durability and structural integrity. Figure 10 presents the FS results of GPC, comparing control and treated samples. The combination of 30% WPA and 3% HDPE significantly influences the FS of GPC, similar to its effects on CS and STS. Control samples have

an FS of 3.38 MPa at 7 days and 4.53 MPa at 28 days, while treated samples demonstrate an improved FS of 3.88 MPa at 7 days and 5.10 MPa at 28 days. This signifies improvements of 14.8% and 12.6% over control samples, respectively. Kangavar et al. [93] confirmed the crack-gathering behavior of HDPE particles in their study of PET granules, which explains the observed rise in FS in treated samples. Under applied loads, HDPE particles efficiently aggregate and consolidate fractures in GPC, leading to enhanced performance. Tamil Selvi et al. [45] discovered that the incorporation of 3% HDPE granules into concrete enhanced FS by 8%, hence supporting the evidence for the efficacy of HDPE. Moreover, the incorporation of WPA imitates its effect on CS, which improves FS. Furthermore, the contribution of WPA is of equivalent importance. WPA induces a pozzolanic reaction that yields C-S-H, C-A-S-H, and N-A-S-H gels, thereby improving the bonding and load-bearing capacity of the GPC. This synergistic gel formation enhances the mechanical qualities and increases the durability of the GPC by decreasing porosity and increasing density. The interaction between WPA and MK results in the formation of these gels, which enhance the FS of GPC [69, 94, 95]. This attribute is especially important in applications exposed to bending loads. The combined effect of HDPE and WPA enhances FS, thereby diminishing cracks and increasing load-bearing capacity in GPC.

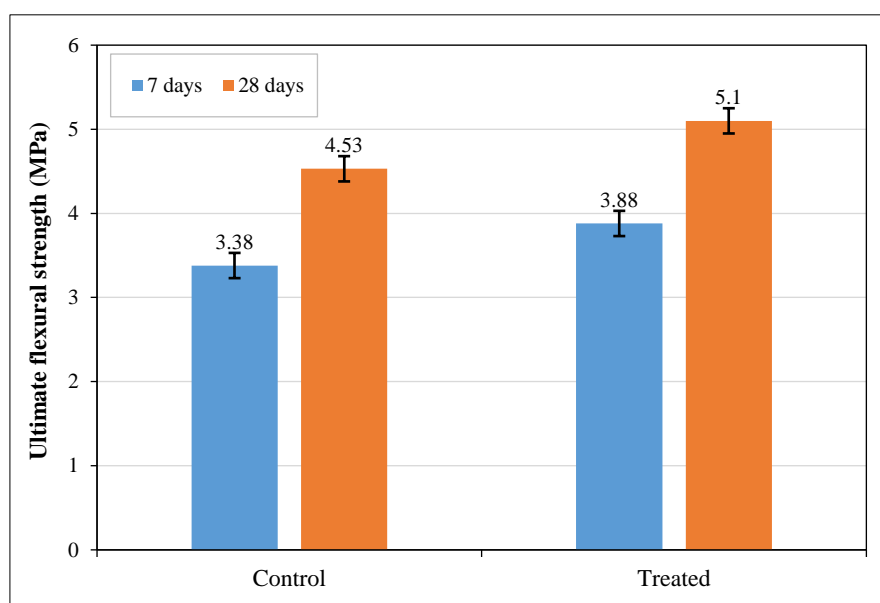


Figure 10. Effect of the treated GPC on the Ultimate FS

3.7. UPV of Control and Treated GPC

The non-destructive UPV testing method was used to assess the strength of GPC in this study, as shown in Figure 11. Initial UPV tests at 7 days revealed that the control sample demonstrated a velocity of 2.71 km/s; however, the treated sample, which included 30%WPA and 3% HDPE, attained a superior velocity of 3.2 km/s, indicating a 18% enhancement. At 28 days, both samples exhibited additional improvements, with UPV values of 3.82 km/s for the control and 4.36 km/s for the treated sample, yielding a 14.12% variance. The UPV results exhibited a significant association with CS test outcomes, highlighting the success of UPV in tracking the strength development of GPC over time. The considerable enhancements in UPV and CS from 7–28 days indicate a continuous strengthening of GPC during the curing process. Adding WPA and HDPE to the treated samples had a big effect on the microstructure of the GPC, making it denser and less porous. This could have made it better at transmitting ultrasonic waves, which led to higher UPV values. Additionally, UPV tests evaluated the quality of GPC in accordance with the BSI B.203: Part 203 [96] standards, providing an accurate basis for determining concrete quality. During the 28-day period, the UPV test classified both the control and treated samples as "good" quality (G), highlighting their satisfactory strength properties and further validating the UPV test's reliability and precision as an evaluative tool for GPC structures. The non-destructive characteristics of the UPV test provide the assessment of GPC's internal properties and overall structural integrity without damaging the samples, making it an economically feasible choice for regular quality control. Furthermore, UPV testing may reveal crucial details about voids, cracks, and delamination, all of which significantly impact the material's durability and long-term effectiveness. Early identification of such weaknesses facilitates prompt adjustments to improve the durability and dependability of GPC structures. The findings confirm that the UPV test is a reliable and efficient non-destructive technique for evaluating the strength characteristics and overall quality of GPC, especially when enhanced by the inclusion of WPA and HDPE, with considerable implications for enhancing the performance and sustainability of GPC in practical applications.

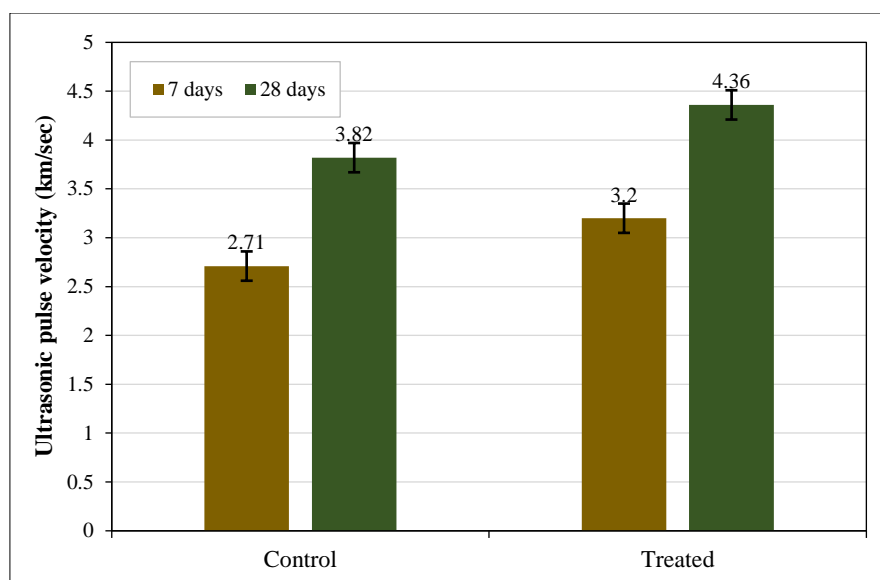


Figure 11. UPV test results of GPC

3.8. Effect of Water Absorption by Curing Ages on of the Control and Treated GPC

The influence of curing age on GPC water absorption is visualized in Figure 12. The findings of the study on water absorption in GPC mixtures demonstrate a correlation with CS. For curing durations of 2, 5, 7, 14, 21, and 28 days, respectively, the control mix achieved water absorption rates of 7.72%, 6.65%, 5.55%, 4.95%, 4.62%, and 4.15%. The treated geopolymer mix, on the other hand, exhibited significantly lower water absorption, with values of 7.15%, 6.12%, 4.95%, 4.42%, 4.05%, and 3.65% over the same curing durations while also achieving superior CS. The different amounts of water absorbed by the two mixtures can be explained by the void content. More voids mean more water absorbed, while the treated geopolymer mix absorbed less water, which suggests a more compact internal structure. The efficacy of geopolymerization in creating a strong matrix with reduced voids is essential, as demonstrated by Albidah et al. [97], which highlights that a properly executed geopolymerization procedure results in a more uniform and cohesive structure. The addition of WPA promotes the development of C-A-S-H gel, resulting in a denser microstructure and pore-filling capacity and thereby decreasing both the water absorption and porosity of GPC [98].

Geopolymerization is the chemical transformation of aluminosilicate minerals into an inorganic, three-dimensional network. Geopolymerization involves the dissolution of calcium-aluminosilicate materials, including MK and WPA, in an alkaline environment, leading to the creation of polymeric geopolymer chains that provide structural stability. An effective geopolymerization method improves the density of the resulting matrix, reduces voids, and promotes CS. Efficient geopolymerization achieves a compact microstructure that significantly reduces water absorption, particularly beneficial for applications that require water resistance. Moreover, reduced water absorption enhances the durability of GPC by minimizing the hazards associated with freeze-thaw cycles, chemical attacks, and moisture-related deterioration. This decrease in water absorption maintains the structural integrity and durability of GPC throughout time. Better geopolymerization creates a denser matrix that makes the GPC stronger and more resistant to cracks. This enhances the structure's overall performance by enabling it to withstand higher external pressures. The use of WPA and HDPE in the geopolymer mixture enhances durability and strength by optimizing the internal structure. Figure 13 shows the relationship between average CS and average water absorption in GPC cubes; the R^2 (coefficient of determination) value for the control is 0.969, while the treated value is 0.9713. Notably, the treated GPC shows a more linear relationship between CS and water absorption than the control.

3.9. Stress-Strain Behavior and Mods of Failure of the Control and Treated GPC Cylinders

The impact of WPA and HDPE granules on the crack behavior of GPC under compressive loading can be assessed by analyzing the failure patterns in relation to the material's stiffness and compressive characteristics. Table 5-a displays the standard stress-strain curves and failure mechanisms observed in control GPC cylinders following a 28-day curing period. Table 5-a details the principal parameters that define the stress-strain response of the 28-day control GPC cylinder. These parameters include the elastic modulus (E), peak CS (σ_p), compressive strain at peak stress (ϵ_p), ultimate compressive strength (σ_u), and compressive strain at ultimate failure (ϵ_u), recorded as 22,150 MPa, 23.22 MPa,

0.002712 mm, 14.224 MPa, and 0.004823 mm, respectively. The ultimate CS was determined to be 38.74% lower than the peak value. Following the compressive failure, the control GPC cylinder displayed vertically oriented cracks. The integration of WPA and HDPE into the GPC mix could prevent cracking under compression, as evidenced by tests performed by Xie et al. [79]. These compounds enhance the endurance and structural integrity of GPC; hence, they diminish crack formation.

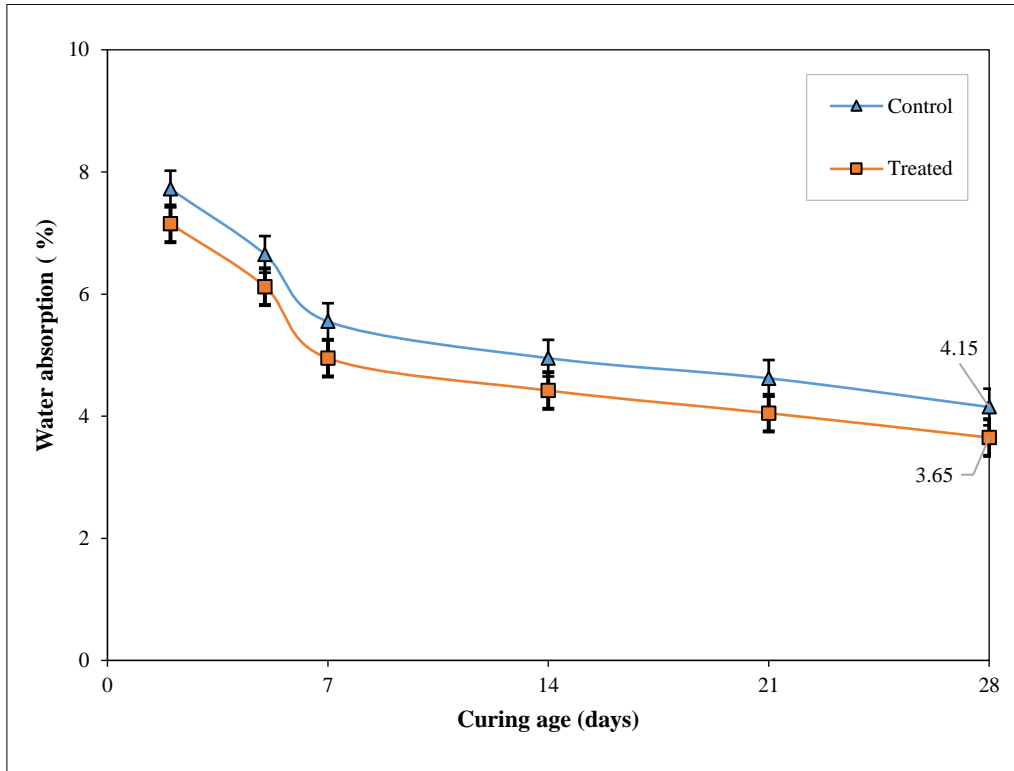


Figure 12. Effect of curing age on water absorption of GPC

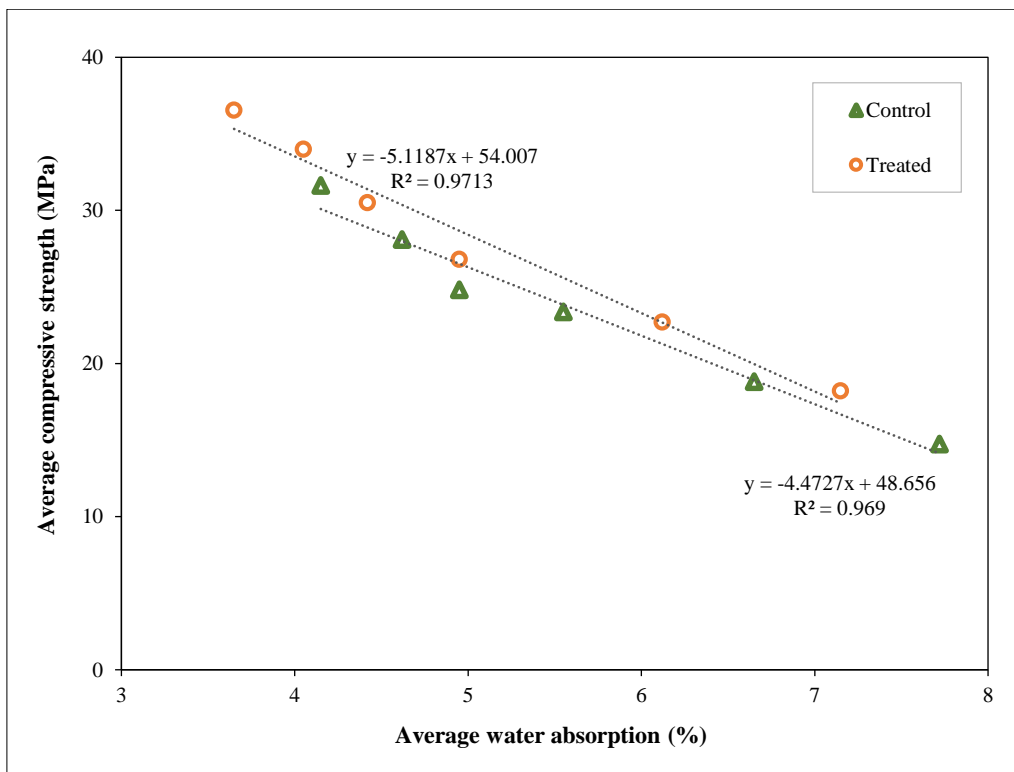


Figure 13. Linear relationship between the average water absorption and average peak CS of the GPC

Table 5. Typical stress-strain curves and modes of failure of 28-days curing age of (a) control GPC cylinder, and (b) treated GPC cylinder

Stress-strain Curve	Failure Mode

Table 5-b displays the characteristic stress-strain curves and modes of failure of GPC cylinders subjected to 30% WPA and 3% HDPE after 28 days of curing. The stress-strain analysis of the treated GPC cylinder at this curing age revealed an E of 24,030 MPa, σ_p of 26.84 MPa, ϵ_p of 0.00233 mm, σ_u of 18.325 MPa, and ϵ_u of 0.005122 mm, as presented in Table 5-b. The E and σ_p of the treated GPC cylinders were significantly superior to those of the control cylinders, signifying improved mechanical performance. The ultimate CS was determined to be 31.73% lower than the peak strength. The treated GPC samples exhibited a lower drop in compressive strength at the equivalent curing age, indicating superior volume stability under compressive stress relative to the controls. The incorporation of WPA and HDPE may have facilitated this enhancement by providing fillers and thus lowering porosity and water absorption. Upon failure, the treated GPC cylinder showed a partially vertical crack, while the control sample displayed a more significant vertical crack, highlighting the enhanced resistance of the treated GPC to cracking under compressive pressure. The variations in the expansion of cracks can be attributed to the microstructural modifications caused by substituting MK with WPA. This substitution facilitates the development of hydration products, including C-A-S-H and N-A-S-H gel matrices, which enhance the internal structure. The creation of a dense gel improves bonding within the GPC matrix and markedly diminishes the possibility of fracture development, as indicated by Xu et al. [99], which noticed comparable enhancements with the incorporation of nano silicate in fly ash-based GPC. The denser gel matrices formed through

geopolymerization serve as barriers, effectively preventing the formation and development of interior fractures. The inclusion of HDPE granules enhances this impact by demonstrating crack-bridging behavior, which confines and inhibits crack expansion [91]. The synergistic action of WPA and HDPE results in a more robust microstructure that minimizes crack development and propagation, improving the durability and structural integrity of the GPC.

Table 5 indicates that the treated GPC displays steeper curves compared to the control group. Increasing the slope of a stress-strain curve is associated with a higher modulus of elasticity (MOE), which enhances the ductility of GPC [100]. Consequently, the treated GPC is anticipated to exhibit strong ductility and resistance to significant damage under conditions of accidental overloading. The area under the stress-strain curve during compression indicates the toughness and energy absorption capacity of the GPC [101-103]. Table 5-b demonstrates that the treated GPC exhibits a greater area under the stress-strain curve compared to the control GPC. Treated GPC exhibits enhanced toughness and energy absorption capacity. Treated GPC exhibits enhanced impact resistance and structural integrity. The stress-strain curve patterns of both mixtures were comparable to those identified by Chitrala et al. [102], Xie et al. [79], and Yadollahi and Benli [104].

3.10. Microstructure and Morphological.

3.10.1. SEM Analysis of Control and Treated GPC

The microstructural properties of control samples comprising only MK and samples incorporating 30% WPA, and 3% HDPE were analyzed using SEM, as depicted in Figure 14. The micrographs illustrate the morphology and density of the microstructure in both material types. Figure 14-a illustrates the microstructure of the control mixture, which is characterized by numerous voids and a relatively low density. The existence of these spaces indicates that the particles exhibit reduced compactness and a diminished degree of interaction. The absence of WPA in the control mixture may have hindered the formation of the C-A-S-H gel. C-A-S-H gel enhances the microstructural density in geopolymer materials. Figure 14-b illustrates the microstructure of the treated sample. This image demonstrates a significant reduction in pore quantity and a more compact microstructure relative to the control mixture. The incorporation of WPA increases the calcium oxide concentration in the mixture, thereby facilitating the formation of the C-A-S-H gel. This gel fills voids and enhances particle bonding, resulting in a dense microstructure. The microstructures of both samples exhibit homogeneity, suggesting an even distribution of the geopolymer matrix within the specimen. Homogeneity is essential for achieving optimal mechanical properties and performance in GPC. According to Ju et al. [105] and Yuan et al. [106], introducing calcium oxide to GPC creates a denser microstructure, and the unhydrated particles were not detected in samples containing calcium hydroxide.

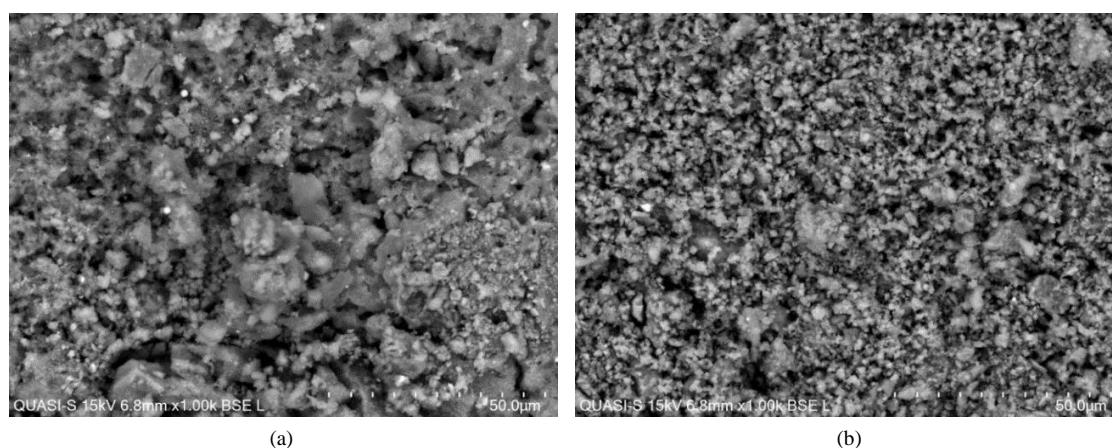


Figure 14. The microstructure of (a) control GPC sample, (b) treated GPC sample

Na_2SiO_3 and $\text{Ca}(\text{OH})_2$ play essential roles in various reactions during the alkaline activation of MK GPC. Na_2SiO_3 , also known as water glass, dissolves in MK, releasing silicate species that interact with aluminum in MK to form an amorphous aluminosilicate gel. This gel serves as the primary binding phase in the gel, offering both strength and stability. When $\text{Ca}(\text{OH})_2$ is mixed with Na_2SiO_3 solution, more C-S-H gel is made. This makes the GPC stronger, durable, and have a denser microstructure. According to the results, the reactions turn MK into a solid, compact substance. This shows how Na_2SiO_3 and $\text{Ca}(\text{OH})_2$ work together to make MK-based systems geopolymerization. Yang et al. [47] demonstrated through SEM analysis that combining $\text{Ca}(\text{OH})_2$ -based GGBS with Na_2SiO_3 resulted in a denser product. The formation of C-S-H gels and smaller hydration products, including C_2ASH_8 and C_4AH_{13} , occurs rapidly, signifying the development of hydration products. The integration of C-S-H and C-A-S-H enhances the efficacy of treated GPC. C-S-H serves as the primary binding phase, enhancing strength and durability while reducing porosity and thereby improving resistance to environmental impacts and cracking. The fibrous structure enhances load-bearing

capacity, facilitating quicker construction through accelerated early strength development. C-A-S-H functions as an additional binding phase, enhancing mechanical properties. The globular shape facilitates the uniform dispersion of binding phases, thereby enhancing the stability and chemical resistance of GPC. The combination of these hydrates produces a synergistic effect, enhancing the strength and durability of treated GPC across various building applications [107].

3.10.2. EDX Analysis of Control and Treated GPC

Figure 15 presents the EDX analysis results for both control and treated GPC samples following a 28-day curing period, indicating notable findings. The principal components of GPC are silicon (Si), calcium (Ca), aluminum (Al), and oxygen (O), with their concentrations detailed in Table 6. These components are crucial for the formation of C-S-H, C-A-S-H, and N-A-S-H gels, which serve as the principal binding phases in GPC. Zhang et al. [108] indicated that these four elements exhibited significant peaks in EDX spectra for concrete containing surface-treated fly ash cenospheres used as internal curing agents. Table 6 indicates that the treated samples exhibited significantly elevated amounts of calcium, silicon, and aluminum, which are crucial for strengthening the production of C-A-S-H gels, essential to improving the mechanical properties of GPC. The treated samples exhibited a combined content of silicon, calcium, aluminum, and oxygen at 84.78%, in contrast to 81.24% in the control samples. The incorporation of WPA facilitates the formation of C-A-S-H gels, as evidenced by the increased element content and improved microstructure of the treated GPC (Figure14-b). These gels diminish porosity and improve the cohesiveness of the treated GPC, resulting in enhanced structural integrity and strength [109, 110].

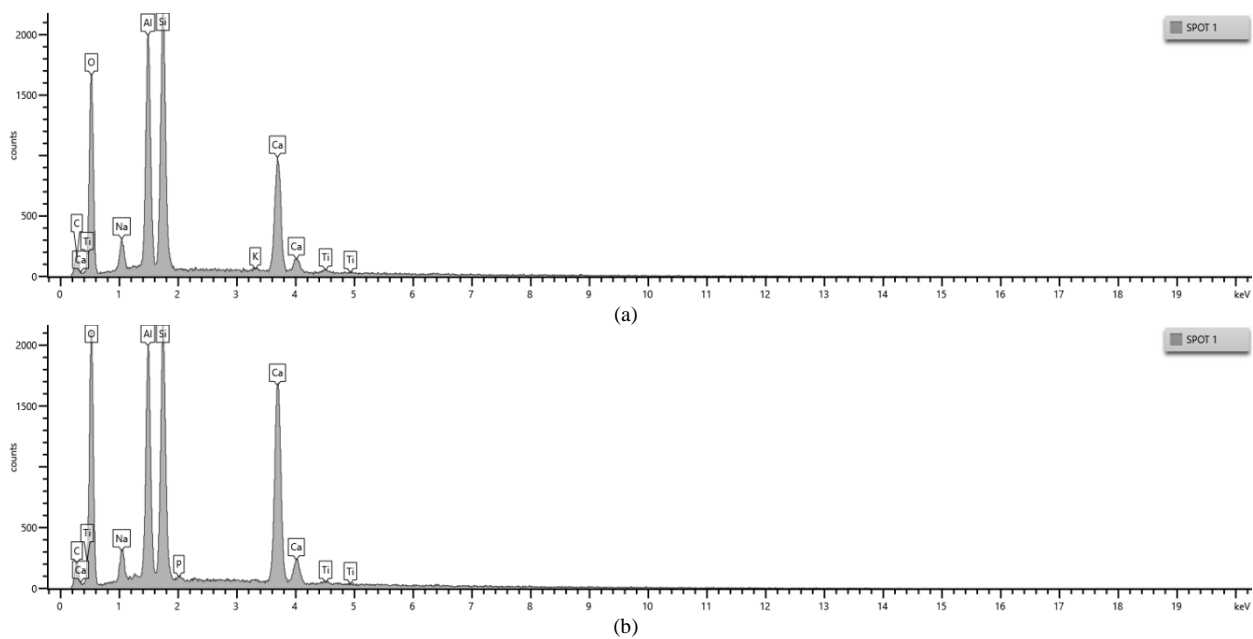


Figure 15. EDX test result of (a) control sample, (b) treated sample

Table 6. Element weights based on the EDX graphical plot of (a) control and (b) treated GPC sample at 28-day

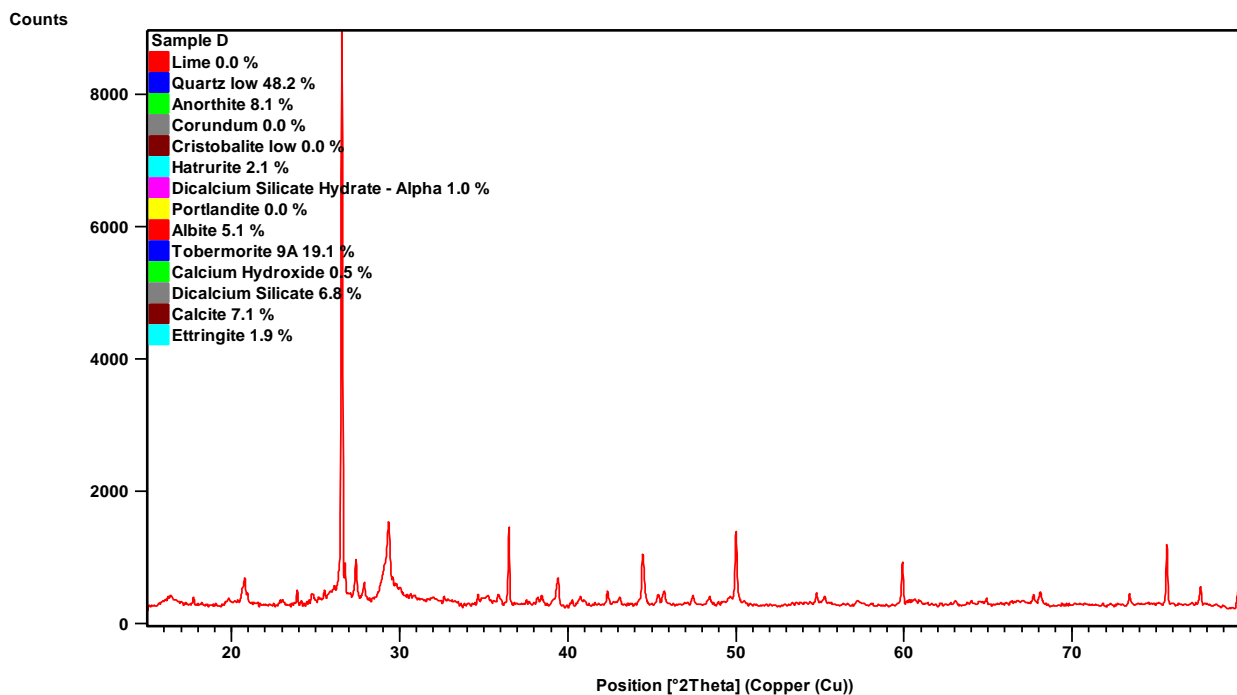
Element	Weight %	
	a	b
Oxide (O)	43.49	46.97
Calcium (Ca)	12.02	17.12
Carbon (C)	15.89	12.53
Aluminum (Al)	11.59	9.66
Silicon (Si)	14.14	11.03
Sodium (Na)	2.17	2.08
Potassium (K)	0.23	NA
Titanium (Ti)	0.47	0.35
Phosphorus (P)	NA	0.26
Total	100.00	100

This study is compatible with the observed mechanical parameters of the GPC mixture. It indicates that higher concentrations of calcium, silicon, and aluminum in treated samples cause the formation of C-A-S-H gel, resulting in improved mechanical performance. The higher calcium concentration in WPA samples is particularly important. Calcium is considered to assist in the formation of additional C-A-S-H gel, hence improving the CS and durability of GPC. The inclusion of WPA, which contains a high calcium concentration, offers a viable method for increasing the mechanical properties of the geopolymer combination. Furthermore, silicon and aluminum in both the control and treated samples are required for the formation of geopolymer gels. These gels act as binding agents, holding the GPC together. However, combining silicon, aluminum, and calcium in treated samples promotes the formation of a more compact and stable gel structure. It is essential to recognize that the mechanical properties of GPC are greatly influenced by the composition of its fundamental components. Increased amounts of calcium, silicon, and aluminum in treated samples enhance the formation of a long-lasting and resistant C-A-S-H gel. This improves the mechanical properties of GPC. The identification of these four elements underscores their critical role in the geopolymerization process.

This highlights the relationship between the elemental composition and the mechanical properties of the mixture. The GPC samples demonstrate the required chemical signatures for effective geopolymerization and mechanical performance, underscoring their suitability for the intended application. The elevated proportion of these elements, along with the uniform and dense microstructures illustrated in Figure 14, suggests the effectiveness of Ca(OH)_2 , MK, and WPA in facilitating the formation of C-S-H and C-A-S-H gels. This process reduces porosity and enhances the strength of the GPC [108]. Furthermore, the similarity of the EDX analysis to the stated mechanical properties indicates the efficacy of the analytical method used in this study. The EDX analysis is an effective tool for assessing the elemental composition of GPC.

3.10.3. XRD Analysis of Control and Treated GPC

After 28 days, the phase composition of GPC specimens containing MK and WPA was determined using XRD. Figure 16 depicts XRD patterns with distinct features in the 2θ range of 25° to 30° , including a significant hump. Quartz, tobermorite, calcite, dicalcium silicate, albite, anorthite, and minor peaks of hatrurite and ettringite were discovered. Further analysis revealed that the control sample had higher peaks for quartz, tobermorite, and dicalcium silicate. In contrast, the sample containing WPA showed greater peaks for anorthite, hatrurite, calcite, and albite. This means that the addition of WPA altered the phase composition of the GPC. The presence of quartz indicates that the reaction between MK's SiO_4 units and the alkaline activator created SiO_2 . This process improves the strength and durability of the GPC. Tobermorite is generated by the reaction of MK and the alkaline activator, adding stability to the concrete structure.



(a)

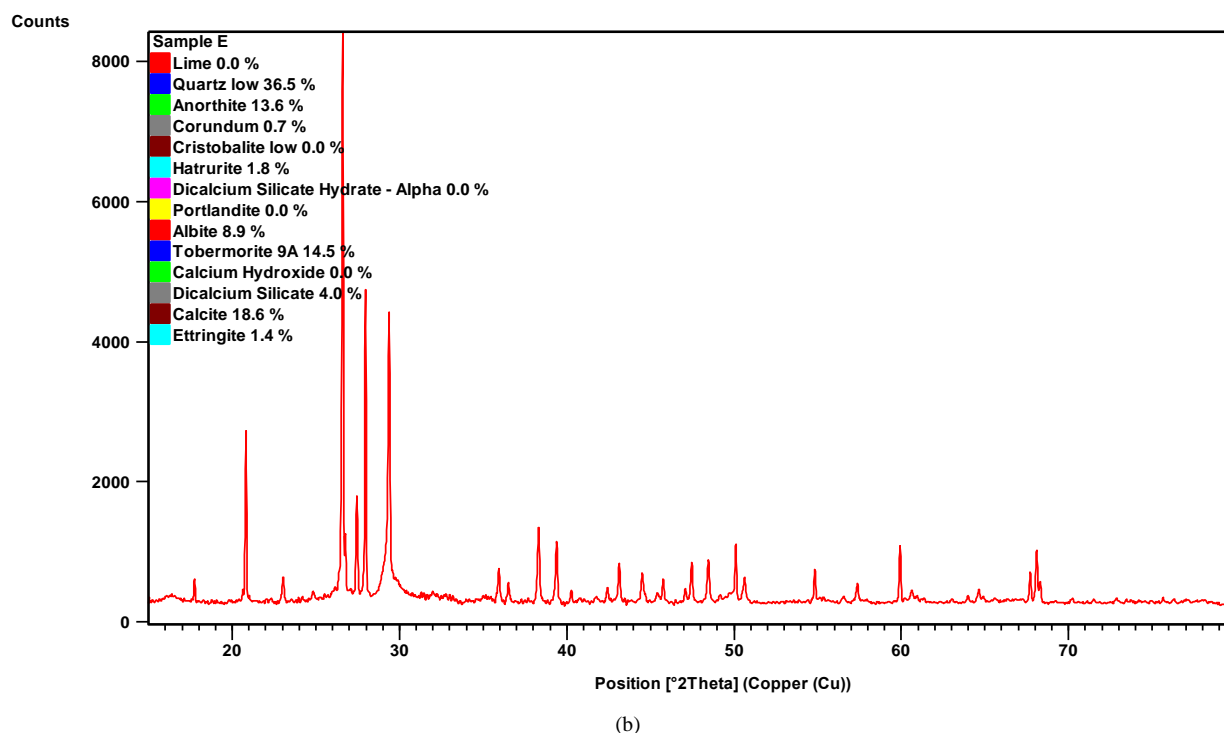


Figure 16. XRD test result of (a) control sample, (b) treated sample

The presence of dicalcium silicate indicates that there is unreacted cementitious material in the geopolymer matrix. This could be due to the incomplete dissolution and reactivity of the precursor components during the geopolymerization process. The greater amount of anorthite peaks in the sample, which included WPA, indicates that the presence of this additional substance promotes the formation of this reaction phase. Anorthite is a calcium-aluminosilicate phase that enhances the mechanical qualities of GPC. Similarly, the greater peaks of hatrurite and calcite in the WPA sample show that the inclusion of this additional material influences these phases as well. Hatrurite is a calcium silicate phase, while calcite is a calcium carbonate phase. Both phases assist in improving the GPC's overall performance and durability. The control and WPA samples both included albite, a sodium feldspar. The peak intensity was higher in the second, indicating that this reaction phase was more common in the geopolymer matrix. The tiny peaks of ettringite indicate the presence of this reaction phase, which improves the GPC's long-term strength and endurance. Ettringite is formed when alumina and sulphate react in a geopolymer matrix.

4. Conclusions

- Incorporating 30% WPA increases the slump compared to the control group. WPA's lower fineness modulus than MK, which leads to less water demand and improved workability of GPC, could be the cause of this increase. Furthermore, combining 3% HDPE and 30% WPA reduced the slump in comparison to 30% WPA mix. The roughness of HDPE particles and their large surface area could cause higher friction between HDPE particles and geopolymer matrices, leading to a loss of workability.
- The use of MK in GPC contributes to its rapid initial and final setting periods. This is mostly due to the high fineness of MK, which shortens the dormant time and accelerates the geopolymerization process, resulting in rapid hardening. As a highly reactive substance, MK aids in the early stages of geopolymerization, leading to faster strength growth and GPC setting. The increased surface area of small particles in MK creates more sites for the geopolymerization reaction to occur, resulting in faster hydration and binding of the ingredients in the GPC mix. Therefore, GPC based on MK has shorter setting durations and greater early strength development, making it useful for construction applications that require rapid setting and early strength. The addition of 30% WPA improves setting times. The quick solidification of WPA in the GPC mix is responsible for this significant performance improvement. The presence of CaO in WPA is higher than in MK, which is the main reason for this improvement.
- The mechanical properties of the control and treated GPC, such as CS, STS, FS, water absorption, and UPV, show a constant improvement with curing age. This indicates that the GPC becomes more resilient as the curing process progresses. Furthermore, the results indicate that using calcium hydroxide as an activator in the MK-based geopolymer improves its properties. The presence of calcium hydroxide enhances the geopolymerization process, resulting in better bonding and strength development in the GPC. The CS data reveal that incorporating 30% WPA shows the best results, whereas replacing 100% WPA results in a higher decrease in CS. The replacement of 30%

of MK with activated WPA optimizes the CS of GPC due to the ideal balance of pozzolanic activity and binder properties. At this level of replacement, the formation of C-A-S-H and N-A-S-H gels greatly improves the microstructure by making it denser and less porous, both of which are necessary for strength under load. Additionally, incorporating 3% HDPE with 30% WPA further boosts CS by improving stress distribution and material flexibility, demonstrating the potential of this GPC mix for sustainable construction applications.

- SEM, EDX, and XRD analysis of treated GPC specimens revealed a significant improvement in pore structure compared to the control group. Furthermore, the treated samples had higher levels of calcium (Ca), silicon (Si), oxygen (O), and aluminum (Al), as well as improved microstructural features. The presence of cementation materials revealed that the treated GPC exhibited more pozzolanic reactions than the control specimens.

Aside from optimizing the mechanical performance of GPC with different proportions of HDPE and WPA, it is recommendable for future research to focus on investigating its long-term durability under various environmental conditions, such as freeze-thaw cycles and exposure to aggressive chemicals. Given HDPE's non-absorptive nature and low density, its influence on pore structure and permeability may affect the material's resistance to these factors. Evaluating these durability aspects will be crucial for a comprehensive understanding of GPC's performance with HDPE, thereby supporting its practical application in diverse environmental conditions.

5. List of Abbreviations

GPC	Geopolymer concrete	SEM	Scanning electron microscopy
WPA	Wastepaper ash	EDX	Energy dispersive X-ray
MK	Metakaolin	XRD	X-ray diffraction
HDPE	High-Density Polyethylene	PC	Portland cement
CS	Compressive strength	GGBS	Ground granulated blast slag
STS	Splitting tensile strength	C-S-H	Calcium-silicate hydrate
FS	Flexural strength	C-A-S-H	Calcium-aluminosilicate hydrate
UPV	Ultrasonic pulse velocity	N-A-S-H	Sodium-aluminosilicate hydrate

6. Declarations

6.1. Author Contributions

Conceptualization, M.A.K.M.; methodology, M.A.K.M.; investigation, M.A.K.M.; writing—original draft preparation, M.A.K.M.; writing—review and editing, L.S.W.; supervision, L.S.W. All authors have read and agreed to the published version of the manuscript.

6.2. Data Availability Statement

The data presented in this study are available on request from the corresponding author.

6.3. Funding and Acknowledgments

The authors would like to show appreciation for the funding related to this academic paper, derived from the research grant known as Fundamental Research Grant Scheme (FRGS), grant number FRGS/1/2022/TK01/UNITEN/02/1, sponsored by the Malaysian Ministry of Higher Education.

6.4. Conflicts of Interest

The authors declare no conflict of interest.

7. References

- [1] Li, H., Deng, Q., Zhang, J., Xia, B., & Skitmore, M. (2019). Assessing the life cycle CO₂ emissions of reinforced concrete structures: Four cases from China. *Journal of Cleaner Production*, 210, 1496–1506. doi:10.1016/j.jclepro.2018.11.102.
- [2] Hendriks, C. A., Worrell, E., Price, L., Martin, N., Ozawa Meida, L., de Jager, D., & Riemer, P. (1999). Emission reduction of greenhouse gases from the cement industry. *Greenhouse Gas Control Technologies* 4, 30, 939–944. doi:10.1016/b978-008043018-8/50150-8.
- [3] Lawrence, C. D. (1998). The Production of Low-Energy Cements. *Lea's Chemistry of Cement and Concrete*, 421–470, Elsevier, Amsterdam, Netherlands. doi:10.1016/b978-075066256-7/50021-7.
- [4] John, S. K., Nadir, Y., & Girija, K. (2021). Effect of source materials, additives on the mechanical properties and durability of fly ash and fly ash-slag geopolymer mortar: A review. *Construction and Building Materials*, 280, 122443. doi:10.1016/j.conbuildmat.2021.122443.

- [5] Davidovits, J. (2013). Geopolymer cement. A review. Geopolymer Institute, Technical papers, 21, Geopolymer Institute Library, Saint-Quentin, France.
- [6] Wetzel, A., & Middendorf, B. (2019). Influence of silica fume on properties of fresh and hardened ultra-high performance concrete based on alkali-activated slag. *Cement and Concrete Composites*, 100, 53–59. doi:10.1016/j.cemconcomp.2019.03.023.
- [7] Cai, R., Wu, T., Fu, C., & Ye, H. (2022). Thermal degradation of potassium-activated ternary slag-fly ash-silica fume binders. *Construction and Building Materials*, 320. doi:10.1016/j.conbuildmat.2021.126304.
- [8] Xu, S., Yuan, P., Liu, J., Pan, Z., Liu, Z., Su, Y., Li, J., & Wu, C. (2021). Development and preliminary mix design of ultra-high-performance concrete based on geopolymer. *Construction and Building Materials*, 308, 125110. doi:10.1016/j.conbuildmat.2021.125110.
- [9] Nair, A. S., Al-Bahry, S., Gathergood, N., Tripathi, B. N., & Sivakumar, N. (2020). Production of microbial lipids from optimized waste office paper hydrolysate, lipid profiling and prediction of biodiesel properties. *Renewable Energy*, 148, 124–134. doi:10.1016/j.renene.2019.12.008.
- [10] Ighalo, J. O., & Adeniyi, A. G. (2020). A perspective on environmental sustainability in the cement industry. *Waste Disposal and Sustainable Energy*, 2(3), 161–164. doi:10.1007/s42768-020-00043-y.
- [11] Ali, A., Hashmi, H. N., & Baig, N. (2013). Treatment of the paper mill effluent-A review. *Annals of the Faculty of Engineering Hunedoara*, 11(3), 337.
- [12] Wang Wang, B., Li, K., Nan, D., Feng, S., Hu, B., Wang, T., & Lu, Q. (2022). Enhanced production of levoglucosenone from pretreatment assisted catalytic pyrolysis of waste paper. *Journal of Analytical and Applied Pyrolysis*, 165, 105567. doi:10.1016/j.jaap.2022.105567.
- [13] Beyene, H. D., Werkneh, A. A., & Ambaye, T. G. (2018). Current updates on waste to energy (WtE) technologies: a review. *Renewable Energy Focus*, 24, 1–11. doi:10.1016/j.ref.2017.11.001.
- [14] Das, S., Lee, S. H., Kumar, P., Kim, K. H., Lee, S. S., & Bhattacharya, S. S. (2019). Solid waste management: Scope and the challenge of sustainability. *Journal of Cleaner Production*, 228, 658–678. doi:10.1016/j.jclepro.2019.04.323.
- [15] Ma, Y., Wang, J., & Zhang, Y. (2017). TG–FTIR study on pyrolysis of waste printing paper. *Journal of Thermal Analysis and Calorimetry*, 129(2), 1225–1232. doi:10.1007/s10973-017-6218-3.
- [16] Solahuddin, B. A., & Yahaya, F. M. (2021). Properties of concrete containing shredded waste paper as an additive. *Materials Today: Proceedings*, 51, 1350–1354. doi:10.1016/j.matpr.2021.11.390.
- [17] Palanichamy, P., Venkatachalam, S., & Gupta, S. (2023). Improved recovery of cellulose nanoparticles from printed wastepaper and its reinforcement in guar gum films. *Biomass Conversion and Biorefinery*, 13(15), 14113–14125. doi:10.1007/s13399-022-02516-y.
- [18] Zhou, R. X., Stanley, R., & Le, M. (2012). Contamination of food with newspaper ink: An evidence-informed decision making (EIDM) case study of homemade dessert. *Environmental Health Review*, 55(02), 63–69. doi:10.5864/d2012-005.
- [19] Duan, H., Zhao, Q., Song, J., & Duan, Z. (2021). Identifying opportunities for initiating waste recycling: Experiences of typical developed countries. *Journal of Cleaner Production*, 324. doi:10.1016/j.jclepro.2021.129190.
- [20] Chen, W., Shi, S., Chen, M., & Zhou, X. (2017). Fast co-pyrolysis of waste newspaper with high-density polyethylene for high yields of alcohols and hydrocarbons. *Waste Management*, 67, 155–162. doi:10.1016/j.wasman.2017.05.032.
- [21] Lakhari, M. T., Bai, Y., Wong, L. S., Paul, S. C., Anggraini, V., & Kong, S. Y. (2022). Mechanical and durability properties of epoxy mortar incorporating coal bottom ash as filler. *Construction and Building Materials*, 315. doi:10.1016/j.conbuildmat.2021.125677.
- [22] Antunes Boca Santa, R. A., Bernardin, A. M., Riella, H. G., & Kuhnen, N. C. (2013). Geopolymer synthesized from bottom coal ash and calcined paper sludge. *Journal of Cleaner Production*, 57, 302–307. doi:10.1016/j.jclepro.2013.05.017.
- [23] Adesanya, E., Ohenoja, K., Luukkonen, T., Kinnunen, P., & Illikainen, M. (2018). One-part geopolymer cement from slag and pretreated paper sludge. *Journal of Cleaner Production*, 185, 168–175. doi:10.1016/j.jclepro.2018.03.007.
- [24] Spathi, C., Young, N., Heng, J. Y. Y., Vandeperre, L. J. M., & Cheeseman, C. R. (2015). A simple method for preparing super-hydrophobic powder from paper sludge ash. *Materials Letters*, 142, 80–83. doi:10.1016/j.matlet.2014.11.123.
- [25] Kim, M. J., & Jeon, J. (2020). Effects of Ca-ligand stability constant and chelating agent concentration on the CO₂ storage using paper sludge ash and chelating agent. *Journal of CO₂ Utilization*, 40. doi:10.1016/j.jcou.2020.101202.
- [26] Yan, S., & Sagoe-Crentsil, K. (2016). Evaluation of fly ash geopolymer mortar incorporating calcined wastepaper sludge. *Journal of Sustainable Cement-Based Materials*, 5(6), 370–380. doi:10.1080/21650373.2016.1174962.

- [27] Sadique, M., Al-Nageim, H., Atherton, W., Seton, L., & Dempster, N. (2019). Analytical investigation of hydration mechanism of a non-Portland binder with waste paper sludge ash. *Construction and Building Materials*, 211, 80–87. doi:10.1016/j.conbuildmat.2019.03.232.
- [28] De Silva, G. S., & De Silva, B. G. N. G. (2023). Run-off water qualities and engineering properties of sustainable paving blocks with combined waste: waste rice husk ash and coal bottom ash. *Innovative Infrastructure Solutions*, 8(6), 165. doi:10.1007/s41062-023-01125-6.
- [29] Luo, Y. P., Yang, L. B., Wang, D., Zhang, Q., Wang, Z. Y., Xing, M. G., Xue, G., Zhang, J., & Liu, Z. (2024). Effect of GGBFS on the mechanical properties of metakaolin-based self-compacting geopolymer concrete. *Journal of Building Engineering*, 96. doi:10.1016/j.job.2024.110501.
- [30] Gopalakrishna, B., & Pasla, D. (2024). Study of Ambient Cured Fly Ash-GGBS-Metakaolin-Based Geopolymers Mortar. *Low Carbon Materials and Technologies for a Sustainable and Resilient Infrastructure. CBKR 2023, Lecture Notes in Civil Engineering*, 440, Springer, Singapore. doi:10.1007/978-981-99-7464-1_3.
- [31] Thakur, M., & Bawa, S. (2024). Evaluation of strength and durability properties of fly ash-based geopolymer concrete containing GGBS and dolomite. *Energy, Ecology and Environment*, 9(3), 256–271. doi:10.1007/s40974-023-00309-1.
- [32] World Green Building Council (2019). *Global Status Report for Buildings and Construction*. World Green Building Council, London, United Kingdom.
- [33] Yan, H., Shen, Q., Fan, L. C. H., Wang, Y., & Zhang, L. (2010). Greenhouse gas emissions in building construction: A case study of One Peking in Hong Kong. *Building and Environment*, 45(4), 949–955. doi:10.1016/j.buildenv.2009.09.014.
- [34] Miller, S. A., Habert, G., Myers, R. J., & Harvey, J. T. (2021). Achieving net zero greenhouse gas emissions in the cement industry via value chain mitigation strategies. *One Earth*, 4(10), 1398–1411. doi:10.1016/j.oneear.2021.09.011.
- [35] Ford, H. V., Jones, N. H., Davies, A. J., Godley, B. J., Jambeck, J. R., Napper, I. E., Suckling, C. C., Williams, G. J., Woodall, L. C., & Koldewey, H. J. (2022). The fundamental links between climate change and marine plastic pollution. *Science of the Total Environment*, 806, 150392. doi:10.1016/j.scitotenv.2021.150392.
- [36] Major, K. (2021). *Plastic Waste and Climate Change—What’s the Connection*. World Wildlife Fund, Gland, Switzerland.
- [37] Kumar, R., Verma, A., Shome, A., Sinha, R., Sinha, S., Jha, P. K., Kumar, R., Kumar, P., Shubham, Das, S., Sharma, P., & Prasad, P. V. V. (2021). Impacts of plastic pollution on ecosystem services, sustainable development goals, and need to focus on circular economy and policy interventions. *Sustainability (Switzerland)*, 13(17), 9963. doi:10.3390/su13179963.
- [38] Zheng, J., & Suh, S. (2019). Strategies to reduce the global carbon footprint of plastics. *Nature Climate Change*, 9(5), 374–378. doi:10.1038/s41558-019-0459-z.
- [39] Stegmann, P., Daioglou, V., Londo, M., van Vuuren, D. P., & Junginger, M. (2022). Plastic futures and their CO₂ emissions. *Nature*, 612(7939), 272–276. doi:10.1038/s41586-022-05422-5.
- [40] Venkatarama Reddy, B. V. (2009). Sustainable materials for low carbon buildings. *International Journal of Low-Carbon Technologies*, 4(3), 175–181. doi:10.1093/ijlct/ctp025.
- [41] Crawford, R. H. (2022). Greenhouse Gas Emissions of Global Construction Industries. *IOP Conference Series: Materials Science and Engineering*, 1218(1), 012047. doi:10.1088/1757-899x/1218/1/012047.
- [42] Abeyasinghe, S., Gunasekara, C., Bandara, C., Nguyen, K., Dissanayake, R., & Mendis, P. (2021). Engineering performance of concrete incorporated with recycled high-density polyethylene (HDPE)—A systematic review. *Polymers*, 13(11), 1885. doi:10.3390/polym13111885.
- [43] Tamrin, Jamal, M., & Ramadhani, P. (2020). The effect of the shape and size of HDPE plastic admixtures on to K125 concrete. *IOP Conference Series: Earth and Environmental Science*, 419(1), 12066. doi:10.1088/1755-1315/419/1/012066.
- [44] Atienza, E. M., De Jesus, R. M., & Ongpeng, J. M. C. (2023). Development of Foam Fly Ash Geopolymer with Recycled High-Density Polyethylene (HDPE) Plastics. *Polymers*, 15(11), 2413. doi:10.3390/polym15112413.
- [45] Tamil Selvi, M., Dasarathy, A. K., & Ponkumar Ilango, S. (2021). Mechanical properties on light weight aggregate concrete using high density polyethylene granules. *Materials Today: Proceedings*, 81(2), 926–930. doi:10.1016/j.matpr.2021.04.302.
- [46] Zhang, H. Y., Kodur, V., Qi, S. L., Cao, L., & Wu, B. (2014). Development of metakaolin-fly ash based geopolymers for fire resistance applications. *Construction and Building Materials*, 55, 38–45. doi:10.1016/j.conbuildmat.2014.01.040.
- [47] Yang, K. H., Cho, A. R., Song, J. K., & Nam, S. H. (2012). Hydration products and strength development of calcium hydroxide-based alkali-activated slag mortars. *Construction and Building Materials*, 29, 410–419. doi:10.1016/j.conbuildmat.2011.10.063.
- [48] Andrew R.M. (2018). Global CO₂ emissions from cement production. *Earth System Science Data*, 10(4), 1–20. doi:10.5281/zenodo.831455.

- [49] Nath, P., & Sarker, P. K. (2017). Flexural strength and elastic modulus of ambient-cured blended low-calcium fly ash geopolymer concrete. *Construction and Building Materials*, 130, 22–31. doi:10.1016/j.conbuildmat.2016.11.034.
- [50] Mohammadhosseini, H., Ngian, S. P., Alyousef, R., & Tahir, M. M. (2021). Synergistic effects of waste plastic food tray as low-cost fibrous materials and palm oil fuel ash on transport properties and drying shrinkage of concrete. *Journal of Building Engineering*, 42, 102826. doi:10.1016/j.job.2021.102826.
- [51] Pacheco-Torgal, F., Cabeza, L. F., Labrincha, J., & De Magalhaes, A. G. (2014). *Eco-efficient construction and building materials: life cycle assessment (LCA), eco-labelling and case studies*. Woodhead Publishing, Sawston, United Kingdom.
- [52] Munir, Q., Abdulkareem, M., Horttanainen, M., & Kärki, T. (2023). A comparative cradle-to-gate life cycle assessment of geopolymer concrete produced from industrial side streams in comparison with traditional concrete. *Science of the Total Environment*, 865, 161230. doi:10.1016/j.scitotenv.2022.161230.
- [53] Cordeiro, G. C., Toledo Filho, R. D., & Fairbairn, E. M. R. (2009). Effect of calcination temperature on the pozzolanic activity of sugar cane bagasse ash. *Construction and Building Materials*, 23(10), 3301–3303. doi:10.1016/j.conbuildmat.2009.02.013.
- [54] Cherian, C., & Siddiqua, S. (2019). Pulp and paper mill fly ash: A review. *Sustainability (Switzerland)*, 11(16), 4394. doi:10.3390/su11164394.
- [55] Midhin, M. A. K., Wong, L. S., & Jasim, A. M. D. A. (2024). Assessing the Influence of Calcium-Based Alkaline Activators and Metakaolin on the Compressive Strength Development of Geopolymer Concrete for Different Mix Design Parameters. *Annales de Chimie: Science Des Matériaux*, 48(5), 667–677. doi:10.18280/acsm.480507.
- [56] ASTM C33/C33M-18. (2023). *Standard Specification for Concrete Aggregates*. ASTM International, Pennsylvania, United States. doi:10.1520/C0033_C0033M-18.
- [57] BS EN 12390-3. (2009). *Testing Hardened Concrete. CS of Test Specimens. Testing Hardened Concrete—Part 3: Compressive Strength of Test Specimens*. British Standard Institute, London, United Kingdom.
- [58] BS EN 12390-6. (2009). *Testing hardened concrete. Tensile splitting strength of test specimens*. British Standard Institute, London, United Kingdom.
- [59] ASTM C293/C293M-16. (2016). *Standard Test Method for Flexural Strength of Concrete (Using Simple Beam with Center-Point Loading)*. ASTM International, Pennsylvania, United States. doi:10.1520/C0293_C0293M-16.
- [60] ASTM C597-16. (2016). *Standard Test Method for Pulse Velocity through Concrete*. ASTM International, Pennsylvania, United States. doi:10.1520/C0597-16.
- [61] ASTM C642-21. (2022). *Standard Test Method for Density, Absorption, and Voids in Hardened Concrete*. ASTM International, Pennsylvania, United States. doi:10.1520/C0642-21.
- [62] Kumar, P., Pankar, C., Manish, D., & Santhi, A. S. (2018). Study of mechanical and microstructural properties of geopolymer concrete with GGBS and Metakaolin. *Materials Today: Proceedings*, 5(14), 28127–28135. doi:10.1016/j.matpr.2018.10.054.
- [63] Vu, C. C., Plé, O., Weiss, J., & Amitrano, D. (2020). Revisiting the concept of characteristic compressive strength of concrete. *Construction and Building Materials*, 263. doi:10.1016/j.conbuildmat.2020.120126.
- [64] Wong, L. S., Oweida, A. F. M., Kong, S. Y., Iqbal, D. M., & Regunathan, P. (2020). The surface coating mechanism of polluted concrete by *Candida ethanolica* induced calcium carbonate mineralization. *Construction and Building Materials*, 257, 119482. doi:10.1016/j.conbuildmat.2020.119482.
- [65] Wang, Z., Zou, D., Liu, T., & Zhou, A. (2021). Influence of paste coating thickness on the compressive strength, permeability, and mesostructure of permeable concrete. *Construction and Building Materials*, 299, 123994. doi:10.1016/j.conbuildmat.2021.123994.
- [66] Fletcher, R. A., MacKenzie, K. J. D., Nicholson, C. L., & Shimada, S. (2005). The composition range of aluminosilicate geopolymers. *Journal of the European Ceramic Society*, 25(9), 1471–1477. doi:10.1016/j.jeurceramsoc.2004.06.001.
- [67] Autef, A., Joussein, E., Gasgnier, G., & Rossignol, S. (2012). Role of the silica source on the geopolymerization rate ALL or. *Journal of Non-Crystalline Solids*, 358(21), 2886–2893. doi:10.1016/j.jnoncrysol.2012.07.015.
- [68] Meko, B., & Ighalo, J. (2021). Utilization of waste paper ash as supplementary cementitious material in C-25 concrete: Evaluation of fresh and hardened properties. *Cogent Engineering*, 8(1), 1938366. doi:10.1080/23311916.2021.1938366.
- [69] Singh, R. P., Vanapalli, K. R., Cheela, V. R. S., Peddiredy, S. R., Sharma, H. B., & Mohanty, B. (2023). Fly ash, GGBS, and silica fume based geopolymer concrete with recycled aggregates: Properties and environmental impacts. *Construction and Building Materials*, 378, 131168. doi:10.1016/j.conbuildmat.2023.131168.
- [70] Singh, R. P., Vanapalli, K. R., Jadda, K., & Mohanty, B. (2024). Durability assessment of fly ash, GGBS, and silica fume based geopolymer concrete with recycled aggregates against acid and sulfate attack. *Journal of Building Engineering*, 82, 108354. doi:10.1016/j.job.2023.108354.

- [71] Rathinam, K., & Kanagarajan, V. (2022). Behaviour of Fly ash and GGBS based Monoblock Prestressed Geopolymer Concrete Composite sleepers. *Materials Today: Proceedings*, 65, 3321–3327. doi:10.1016/j.matpr.2022.05.406.
- [72] Bouaissi, A., Li, L. yuan, Al Bakri Abdullah, M. M., & Bui, Q. B. (2019). Mechanical properties and microstructure analysis of FA-GGBS-HMNS based geopolymer concrete. *Construction and Building Materials*, 210, 198–209. doi:10.1016/j.conbuildmat.2019.03.202.
- [73] Gao, X., Yu, Q. L., & Brouwers, H. J. H. (2015). Properties of alkali activated slag-fly ash blends with limestone addition. *Cement and Concrete Composites*, 59, 119–128. doi:10.1016/j.cemconcomp.2015.01.007.
- [74] Prusty, J. K., & Pradhan, B. (2020). Effect of GGBS and chloride on compressive strength and corrosion performance of steel in fly ash-GGBS based geopolymer concrete. *Materials Today: Proceedings*, 32, 850–855. doi:10.1016/j.matpr.2020.04.210.
- [75] Dawood, A. O., AL-Khazraji, H., & Falih, R. S. (2021). Physical and mechanical properties of concrete containing PET wastes as a partial replacement for fine aggregates. *Case Studies in Construction Materials*, 14, 482. doi:10.1016/j.cscm.2020.e00482.
- [76] Ismail, Z. Z., & AL-Hashmi, E. A. (2008). Use of waste plastic in concrete mixture as aggregate replacement. *Waste Management*, 28(11), 2041–2047. doi:10.1016/j.wasman.2007.08.023.
- [77] Jindal, B. B., Singhal, D., Sharma, S. K., & Ashish, D. K. (2017). Improving CS of low calcium fly ash GPC with alccofine. *Advances in Concrete Construction*, 5(1), 17. doi:10.12989/acc.2017.19.2.017.
- [78] Waqas, R. M., Butt, F., Zhu, X., Jiang, T., & Tufail, R. F. (2021). A comprehensive study on the factors affecting the workability and mechanical properties of ambient cured fly ash and slag based geopolymer concrete. *Applied Sciences (Switzerland)*, 11(18), 8722. doi:10.3390/app11188722.
- [79] Xie, J., Wang, J., Rao, R., Wang, C., & Fang, C. (2019). Effects of combined usage of GGBS and fly ash on workability and mechanical properties of alkali activated geopolymer concrete with recycled aggregate. *Composites Part B: Engineering*, 164, 179–190. doi:10.1016/j.compositesb.2018.11.067.
- [80] Lee, W. K. W., & Van Deventer, J. S. J. (2002). The effect of ionic contaminants on the early-age properties of alkali-activated fly ash-based cements. *Cement and Concrete Research*, 32(4), 577–584. doi:10.1016/S0008-8846(01)00724-4.
- [81] Hadi, M. N. S., Zhang, H., & Parkinson, S. (2019). Optimum mix design of geopolymer pastes and concretes cured in ambient condition based on compressive strength, setting time and workability. *Journal of Building Engineering*, 23, 301–313. doi:10.1016/j.jobe.2019.02.006.
- [82] Nath, P., & Sarker, P. K. (2014). Effect of GGBFS on setting, workability and early strength properties of fly ash geopolymer concrete cured in ambient condition. *Construction and Building Materials*, 66, 163–171. doi:10.1016/j.conbuildmat.2014.05.080.
- [83] Poloju, K. K., & Srinivasu, K. (2020). Impact of GGBS and strength ratio on mechanical properties of geopolymer concrete under ambient curing and oven curing. *Materials Today: Proceedings*, 42, 962–968. doi:10.1016/j.matpr.2020.11.934.
- [84] Pawluczuk, E., Kalinowska-Wichrowska, K., Jiménez, J. R., Fernández-Rodríguez, J. M., & Suescum-Morales, D. (2021). Geopolymer concrete with treated recycled aggregates: Macro and microstructural behavior. *Journal of Building Engineering*, 44, 103317. doi:10.1016/j.jobe.2021.103317.
- [85] Shilar, F. A., Ganachari, S. V., Patil, V. B., Neelakanta Reddy, I., & Shim, J. (2023). Preparation and validation of sustainable metakaolin based geopolymer concrete for structural application. *Construction and Building Materials*, 371, 130688. doi:10.1016/j.conbuildmat.2023.130688.
- [86] Deb, P. S., Nath, P., & Sarker, P. K. (2014). The effects of ground granulated blast-furnace slag blending with fly ash and activator content on the workability and strength properties of geopolymer concrete cured at ambient temperature. *Materials and Design*, 62, 32–39. doi:10.1016/j.matdes.2014.05.001.
- [87] Matakah, F., Aqel, R., & Ababneh, A. (2020). Enhancement of the Mechanical Properties of Kaolin Geopolymer Using Sodium Hydroxide and Calcium Oxide. *Procedia Manufacturing*, 44, 164–171. doi:10.1016/j.promfg.2020.02.218.
- [88] Yip, C. K., Lukey, G. C., & Van Deventer, J. S. J. (2005). The coexistence of geopolymeric gel and calcium silicate hydrate at the early stage of alkaline activation. *Cement and Concrete Research*, 35(9), 1688–1697. doi:10.1016/j.cemconres.2004.10.042.
- [89] Garcia-Lodeiro, I., Palomo, A., Fernández-Jiménez, A., & MacPhee, D. E. (2011). Compatibility studies between N-A-S-H and C-A-S-H gels. Study in the ternary diagram Na₂O-CaO-Al₂O₃-SiO₂-H₂O. *Cement and Concrete Research*, 41(9), 923–931. doi:10.1016/j.cemconres.2011.05.006.
- [90] Zhao, X., Liu, C., Zuo, L., Wang, L., Zhu, Q., & Wang, M. (2019). Investigation into the effect of calcium on the existence form of geopolymerized gel product of fly ash based geopolymers. *Cement and Concrete Composites*, 103, 279–292. doi:10.1016/j.cemconcomp.2018.11.019.
- [91] Rahim, N. L., Salehuddin, S., Ibrahim, N. M., Amat, R. C., & Ab Jalil, M. F. (2013). Use of plastic waste (high density polyethylene) in concrete mixture as aggregate replacement. *Advanced Materials Research*, 701, 265–269. doi:10.4028/www.scientific.net/AMR.701.265.

- [92] Santhi, Mh., & Santhi, H. M. (2017). Strength and Chloride Permeable Properties of Concrete with High Density Polyethylene Waste. Article in International Journal of Chemical Sciences, 15(1), 108.
- [93] Kangavar, M. E., Lokuge, W., Manalo, A., Karunasena, W., & Frigione, M. (2022). Investigation on the properties of concrete with recycled polyethylene terephthalate (PET) granules as fine aggregate replacement. Case Studies in Construction Materials, 16, 934. doi:10.1016/j.cscm.2022.e00934.
- [94] Parashar, A. K., Sharma, P., & Sharma, N. (2022). Effect on the strength of GGBS and fly ash based geopolymer concrete. Materials Today: Proceedings, 62, 4130–4133. doi:10.1016/j.matpr.2022.04.662.
- [95] Saxena, A., Sulaiman, S. S., Shariq, M., & Ansari, M. A. (2023). Experimental and analytical investigation of concrete properties made with recycled coarse aggregate and bottom ash. Innovative Infrastructure Solutions, 8(7), 197. doi:10.1007/s41062-023-01165-y.
- [96] BS 1881-125. (1986). Testing Concrete Part 203. Recommendations for measurement of velocity of ultrasonic pulses in concrete. In Construction Standard (Vol. 2, Issue 2, pp. 1–14).
- [97] Albidah, A., Alqarni, A. S., Abbas, H., Almusallam, T., & Al-Salloum, Y. (2022). Behavior of Metakaolin-Based geopolymer concrete at ambient and elevated temperatures. Construction and Building Materials, 317. doi:10.1016/j.conbuildmat.2021.125910.
- [98] Bellum, R. R., Muniraj, K., & Madduru, S. R. C. (2020). Influence of slag on mechanical and durability properties of fly ash-based geopolymer concrete. Journal of the Korean Ceramic Society, 57(5), 530–545. doi:10.1007/s43207-020-00056-7.
- [99] Xu, Z., Long, H., Liu, Q., Yu, H., Zhang, X., & Hui, D. (2023). Mechanical properties and durability of geopolymer concrete based on fly ash and coal gangue under different dosage and particle size of nano silica. Construction and Building Materials, 387, 131622. doi:10.1016/j.conbuildmat.2023.131622.
- [100] Lim, J. C., & Ozbakkaloglu, T. (2015). Influence of concrete age on stress-strain behavior of FRP-confined normal- and high-strength concrete. Construction and Building Materials, 82, 61–70. doi:10.1016/j.conbuildmat.2015.02.020.
- [101] Gao, D., Zhang, L., & Nokken, M. (2017). Compressive behavior of steel fiber reinforced recycled coarse aggregate concrete designed with equivalent cubic compressive strength. Construction and Building Materials, 141, 235–244. doi:10.1016/j.conbuildmat.2017.02.136.
- [102] Chitrana, S., Jadaprolu, G. J., & Chundupalli, S. (2018). Study and predicting the stress-strain characteristics of geopolymer concrete under compression. Case Studies in Construction Materials, 8, 172–192. doi:10.1016/j.cscm.2018.01.010.
- [103] Biswal, U. S., Mishra, M., Singh, M. K., & Pasla, D. (2022). Experimental investigation and comparative machine learning prediction of the compressive strength of recycled aggregate concrete incorporated with fly ash, GGBS, and metakaolin. Innovative Infrastructure Solutions, 7(4), 242. doi:10.1007/s41062-022-00844-6.
- [104] Yadollahi, M. M., & Benli, A. (2017). Stress-strain behavior of geopolymer under uniaxial compression. Computers and Concrete, 20(4), 381–389. doi:10.12989/cac.2017.20.4.381.
- [105] Ju, C., Liu, Y., Jia, M., Yu, K., Yu, Z., & Yang, Y. (2020). Effect of calcium oxide on mechanical properties and microstructure of alkali-activated slag composites at sub-zero temperature. Journal of Building Engineering, 32, 101561. doi:10.1016/j.job.2020.101561.
- [106] Yuan, X. H., Chen, W., Lu, Z. A., & Chen, H. (2014). Shrinkage compensation of alkali-activated slag concrete and microstructural analysis. Construction and Building Materials, 66, 422–428. doi:10.1016/j.conbuildmat.2014.05.085.
- [107] Verma, M., Dev, N., Rahman, I., Nigam, M., Ahmed, M., & Mallick, J. (2022). Geopolymer Concrete: A Material for Sustainable Development in Indian Construction Industries. Crystals, 12(4), 514. doi:10.3390/cryst12040514.
- [108] Zhang, Y., Fan, Z., Sun, X., & Zhu, X. (2022). Utilization of surface-modified fly ash cenosphere waste as an internal curing material to intensify concrete performance. Journal of Cleaner Production, 358. doi:10.1016/j.jclepro.2022.132042.
- [109] Wong, L. S., Chandran, S. N., Rajasekar, R. R., & Kong, S. Y. (2022). Pozzolanic characterization of waste newspaper ash as a supplementary cementing material of concrete cylinders. Case Studies in Construction Materials, 17, 1342. doi:10.1016/j.cscm.2022.e01342.
- [110] Midhin, M. A. K., Wong, L. S., Ahmed, A. N., Jasim, A. M. D. A., & Paul, S. C. (2023). Strength and Chemical Characterization of Ultra High-Performance Geopolymer Concrete: A Coherent Evaluation. Civil Engineering Journal (Iran), 9(12), 3254–3277. doi:10.28991/CEJ-2023-09-12-020.